

## 6. UPPER CRETACEOUS CALCAREOUS NANNOFOSSIL BIOSTRATIGRAPHY, ODP LEG 198 (SHATSKY RISE, NORTHWEST PACIFIC OCEAN)<sup>1</sup>

Jackie A. Lees<sup>2</sup> and Paul R. Bown<sup>2</sup>

### ABSTRACT

Eight sites were drilled on Shatsky Rise during Ocean Drilling Program Leg 198. All sites (1207–1214) recovered Cretaceous sediments ranging in age from Maastrichtian to Berriasian. In the Upper Cretaceous, Maastrichtian–Campanian nannofossil oozes were recovered at Sites 1207–1212. At Sites 1207 and 1212 Santonian–Cenomanian oozes were also recovered from chert-dominated sequences, but this interval contains multiple hiatuses. Sites 1209–1211 terminated in chert. Calcareous nannofossil assemblages are abundant, diverse, and relatively well preserved throughout, but biostratigraphy is problematic in places due to missing or rare and sporadically distributed marker species. In the upper Maastrichtian, the first occurrences (FOs) of *Micula murus* and *Lithrathidites quadratus* appear to be reversed in most sections, and in the Campanian, *Reinhardtites levis*, *Misceomarginatus pleniporus*, and *Eiffellithus parallelus* are absent or virtually absent, probably due to biogeographic limitations. However, a number of previously unused bioevents were recognized that may prove to be useful Pacific-wide, including the FO of *Ceratolithoides ultimus* (in Subzone UC20d<sup>TP</sup>) and the last occurrence (LO) of *Tegumentum stradneri* (in Subzone UC20b<sup>TP</sup>) in the upper Maastrichtian; the FOs of *Micula praemurus* and consistent *Cribracorona gallica*, the LOs of *Zeugrhabdotus bicrescenticus* and *Cribracorona echinus*, and the FO of *C. echinus* lower in the Maastrichtian; and the LO of *Rucinolithus? magnus* (in Zone UC16), FO of *R.? magnus* (in Subzone UC15b<sup>TP</sup>), FO of *Perchnielsenella stradneri* (in Subzone UC15a/b<sup>TP</sup>), and

<sup>1</sup>Lees, J.A., and Bown, P.R., 2005. Upper Cretaceous calcareous nannofossil biostratigraphy, ODP Leg 198 (Shatsky Rise, northwest Pacific Ocean). In Bralower, T.J., Premoli Silva, I., and Malone, M.J. (Eds.), *Proc. ODP, Sci. Results*, 198, 1–60 [Online]. Available from World Wide Web: <[http://www-odp.tamu.edu/publications/198\\_SR/VOLUME/CHAPTERS/114.PDF](http://www-odp.tamu.edu/publications/198_SR/VOLUME/CHAPTERS/114.PDF)>. [Cited YYYY-MM-DD]

<sup>2</sup>Department of Earth Sciences, University College London, Gower Street, London WC1E 6BT, United Kingdom. Correspondence author: [j.lees@ucl.ac.uk](mailto:j.lees@ucl.ac.uk)

Initial receipt: 16 March 2004  
Acceptance: 25 February 2005  
Web publication: 13 December 2005  
Ms 198SR-114

FO of *Ceratolithoides indiensis* (Subzone UC14d–UC15d<sup>TP</sup>) in the Campanian.

The assemblages are distinctly different in composition from those of the Atlantic Ocean and its marginal basins but show similarities with some Indian Ocean nannofloras, and so these sections will provide important insights into the paleobiogeography and paleoecology of Late Cretaceous nannoplankton. The assemblages are broadly dominated by cosmopolitan taxa such as *Prediscosphaera*, *Watznaueria*, and *Retecapsa*, but abundance data together with key occurrences and absences reveal a distinct paleobiogeographic character. High-latitude species such as *Seribiscutum primitivum*, *Repagulum parvidentatum*, and *Nephrolithus frequens* are completely absent from the Shatsky sites. The common presence of *Ceratolithoides*, *Uniplanarius*, *Micula*, and *Cylindralithus/Perchmielsenella* are indicative of tropical to subtropical paleolatitudes and reflect an open-ocean setting.

## INTRODUCTION

All eight sites (1207–1214) drilled on Shatsky Rise during Ocean Drilling Program (ODP) Leg 198 recovered Cretaceous sediments that range in age from Berriasian to Maastrichtian. Maastrichtian–Campanian sediments predominantly composed of pure, white nannofossil ooze were recovered at six of the sites (1207–1212); drilling at three of these (Sites 1209–1211) was terminated due to increasing amounts of chert, and at four sites (1208 and 1212–1214) hiatuses were encountered that incorporate much of the pre-Campanian Upper Cretaceous. Turonian and Coniacian sediments appear to have been recovered at Sites 1207 and 1212, but recovery was extremely poor due to pervasive chert beds and apparent hiatuses. At five sites (1207, 1208, and 1212–1214) chert, porcellanite, and nannofossil ooze-dominated mid-Cretaceous sections (Aptian–Cenomanian) were cored, and at Site 1213 a complete Berriasian–Hauterivian section was additionally recovered (Bralower, Premoli Silva, Malone, et al., 2002; **Bown**, this volume). The Shatsky Rise sites include a number of scientifically significant Cretaceous intervals, including four complete Cretaceous/Tertiary (K/T) boundary sections, four mid-Maastrichtian Event (MME) sections, three Oceanic Anoxic Event (OAE) 1a sections, and two OAE1b sections (Bralower, Premoli Silva, Malone, et al., 2002; **Bown**, this volume; Frank et al., 2005; Robinson et al., 2004).

This paper presents the results of shore-based calcareous nannofossil biostratigraphy of the Upper Cretaceous sites (1207–1213), represented by 409 samples. The paper particularly focuses on the Campanian–Maastrichtian interval that forms the bulk of the Upper Cretaceous sediments recovered during Leg 198. Nannofossil assemblages are abundant, diverse, and relatively well preserved throughout, but biostratigraphy is problematic in places due to missing or rare and sporadically distributed marker species. The assemblages are distinctly different in composition from those of the better known Atlantic Ocean and its marginal basins but show similarities with certain Indian Ocean nannofloras. Consequently, the sections provide important insights into the paleobiogeography and paleoecology of Late Cretaceous nannoplankton. The Lower to mid-Cretaceous nannofossil biostratigraphy (Berriasian–Cenomanian) is documented in **Bown** (this volume), the MME in Frank et al. (2005), and the K/T boundary section in **Bown** (in press) and **Premoli Silva et al.** (this volume).

## MATERIAL AND GEOLOGICAL SETTING

Shatsky Rise is a moderate-sized large igneous province that erupted episodically at a hotspot triple-junction intersection between 146 and 133 Ma (Tithonian–Valanginian) at equatorial latitudes (Bralower, Premoli Silva, Malone, et al., 2002). Subsidence of the rise occurred soon after its construction, and Cretaceous water depths were probably on the order of 1.0–2.3 km (Bralower, Premoli Silva, Malone, et al., 2002). The sites were thus above the calcite compensation depth throughout the Cretaceous. Shatsky Rise was located close to the equator in the Early Cretaceous but drifted northward through the Late Cretaceous, and the cessation of chert deposition in the Campanian has been used to argue that Shatsky exited a broad, high-productivity equatorial divergence zone at this time (Bralower, Premoli Silva, Malone, et al., 2002).

Site 1207 is located on the previously undrilled Northern High, Site 1208 on the undrilled Central High, and Sites 1209–1214 on the Southern High of Shatsky Rise (Fig. F1). The Southern High was previously drilled during Deep Sea Drilling Project (DSDP) Legs 6, 32, and 86 and ODP Leg 132, with some Upper Cretaceous sediment recovered at Sites 47, 48, 305, 577, and 810. The Cretaceous sections recovered at all sites during Leg 198 were characterized by pure nannofossil ooze in the Campanian and Maastrichtian and chert with nannofossil ooze and porcellanite in the older Cretaceous sections. The presence of ubiquitous and abundant chert greatly affected core recovery below the Campanian (Bralower, Premoli Silva, Malone, et al., 2002). Nevertheless, almost every core produced some sediment, usually chert or porcellanite, accompanied by layers or vugs of variably lithified nannofossil-rich carbonate. Accordingly, a continuous nannoplankton record was generated through these intervals, but sample spacing is often limited to 9–10 m, and the paucity of carbonate sediment available generally prohibited the recovery of foraminifers (Bralower, Premoli Silva, Malone, et al., 2002).

## METHODS

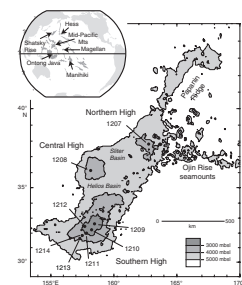
Calcareous nannofossils were analyzed using simple smear slides and standard light-microscope techniques (Bown and Young, 1998). Samples were analyzed semiquantitatively; abundance and preservation categories are given in Table T1. Biostratigraphy is described with reference to both the global Upper Cretaceous UC biozonation of Burnett (1998) and the older CC biozonation of Sissingh (1977, 1978), as modified by Perch-Nielsen (1979, 1983, 1985).

## NANNOFOSSIL RESULTS

### Site 1207

A total of 32 smear slides were examined from Hole 1207A (Cores 198-1207A-18H to 24X, excluding Core 22X, which had no recovery) and 45 from Hole 1207B (Cores 198-1207B-2R through 28R, except Cores 7R [no recovery] and 25R to 27R [chert without adhering calcareous material]). The majority of these nannofossil ooze samples contained moderately well preserved, highly abundant nannofloras. Samples with poor preservation are generally those comprising scrap-

F1. Bathymetric map of Shatsky Rise, p. 27.



T1. Range chart, Hole 1207A, p. 29.

ings from chert pieces. These were analyzed from chert intervals, where core recovery was very low, and the only calcareous material available for analysis was that adhering to the chert (e.g., lower Campanian–middle Coniacian of Hole 1207B; Sections 198-1207B-10R-CC to 19R-CC).

Nannofossil range charts for these holes are shown in Tables T1 and T2. From these, it can be seen that Hole 1207A ranges from upper (Subzones UC15d<sup>TP</sup>–UC15e<sup>TP</sup>) to lower (Subzones UC14d<sup>TP</sup>–UC15a<sup>TP</sup>) Campanian (equivalent to CC22a–CC22c to CC18c–CC19b), terminating in chert, whereas Hole 1207B is upper Campanian (Subzones UC15d<sup>TP</sup>–UC15e<sup>TP</sup>; CC22a–CC22c) to uppermost Albian–lower Cenomanian (Subzones UC0a–UC1a; CC9a–CC9c) (see Bown, this volume, for the Lower Cretaceous succession in this hole). The absence of certain Campanian marker species (*Eiffelithus parallelus*, *Misceomarginatus pleniporus*, and *Bukryaster hayi*) from both holes is discussed below (see “Discussion,” p. 7).

In Hole 1207B, biostratigraphic application was hampered from the pre-Campanian to the upper Coniacian (Subzones UC14c<sup>TP</sup>–UC11b; CC18b–CC14; Sections 198-1207B-10R-CC to 14R-CC) by poorly preserved assemblages from the ooze scrapings from chert pieces, in which only the more robust taxa were present. In the upper–middle Coniacian (Subzone UC11a–Zone UC10; CC18b–CC14; Sections 198-1207B-15R-CC to 19R-CC), *Lithastrinus grillii* was absent, so the UC10/UC11 (CC14/CC15) zonal boundary could not be determined. Zone UC9 (upper Coniacian–middle Turonian; CC13b) appears to be missing, due to very low core recovery combined with the absence from the region, or very sporadic occurrence, of the marker taxa (*Broinsonia parca expansa*, *Zeugrhabdotus biporatus*, and *Lithastrinus septenarius*). A hiatus is not necessarily indicated at this level. Subzones UC8b and UC8a (Sections 198-1207B-20R-CC to 21R-CC; CC13a–CC12) could not be separated because the marker species (*Lucianorhabdus quadrifidus*) is absent from the region. The concentration of first and last occurrences in Section 198-1207B-21R-CC may indicate a hiatus, resulting in the loss of sediments comprising Zone UC7–Subzone UC3d (lower Turonian–upper Cenomanian; CC11–CC10a). The last occurrence (LO) of *Staurolithites gausorhethium* is lower than expected, so Subzones UC3b and UC3c (in CC10a; upper–middle Cenomanian; Section 198-1207B-21R-CC) cannot be separated. Subzones UC2c–UC2b (in CC9c) are missing and Subzones UC1b–UC2a (in CC9c) are indistinguishable because of the presence of a condensed section. The absence from the region of a number of consecutive marker taxa (*Corollithion kennedyi*, *Calculites anfractus*, and *Hayesites albiensis*) means that Subzones UC1a–UC0b (CC9c–CC9b; lower Cenomanian–uppermost Albian; Section 198-1207B-24R-CC) cannot be separated.

### Site 1208

Only one hole was drilled at Site 1208; 43 samples were examined for nannofossils (Cores 198-1208A-36X to 41X; Core 42X had low recovery because of chert, which resulted in termination of the hole). Preservation was generally moderate; nannofossil abundance was generally high. Table T3 shows the nannofossil stratigraphic distributions. The succession is upper (Subzones UC15e<sup>TP</sup>–UC15d<sup>TP</sup>; CC22c–CC22a) to lower (Subzones UC14c<sup>TP</sup>–UC14b<sup>TP</sup>; CC18b) Campanian. Subzones UC15d<sup>TP</sup>–UC15e<sup>TP</sup>, UC14d<sup>TP</sup>–UC15a<sup>TP</sup>, and UC14b<sup>TP</sup>–UC14c<sup>TP</sup> could not be differentiated due to the respective absences of the subzonal markers

---

T2. Range chart, Hole 1207B, p. 30.

---

---

T3. Range chart, Hole 1208A, p. 31.

---

*E. parallelus* (from this site), *M. pleniporus*, and *B. hayi* (from this region) (see “**Discussion**,” p. 7).

### Site 1209

A total of 16 smear slides were examined from Hole 1209A (Cores 198-1209A-25H to 28X, where the hole terminates) and 39 from Hole 1209C (Cores 198-1209C-16H to 22H; there was no recovery from Core 23X, where the hole terminated). Preservation was moderate and abundance high virtually throughout. Tables **T4** and **T5** illustrate the nannofossil stratigraphic distributions. The Hole 1209A succession is upper Maastrichtian (Subzones UC20d<sup>TP</sup>–UC20b<sup>TP</sup>; CC26b–CC25c). Hole 1209C is upper Maastrichtian to around the Maastrichtian/Campanian boundary (Subzone UC20c<sup>TP</sup>–Zone UC17; CC26a–CC23b). Stratigraphic difficulties were encountered in Hole 1209C in differentiating between Zone UC18–Subzone UC20a<sup>TP</sup>, due to the absence of *Reinhardtites levis* from and the higher than expected first occurrence (FO) of *Lithraphidites quadratus* at this location (see “**Discussion**,” p. 7). The uppermost Maastrichtian is present in Hole 1209A, as evidenced by the presence of *Micula prinsii* and *Ceratolithoides ultimus*. Bown (in press) presents the complete K/T interval boundary nannofossil data from this site.

The MME lies between Sections 198-1209C-21H-1, 125 cm, and 21H-3, 128 cm (279.15–282.18 meters below seafloor [mbsf]) (Frank et al., 2005). This interval contains the LO of *Zeughrabdodus bicrescenticus* and lies above the LOs of *Cribracorona echinus* and *Tranolithus orionatus*, in the undifferentiated Zone UC18–Subzone UC20a<sup>TP</sup> (CC24–CC25b).

### Site 1210

A total of 23 samples were analyzed from Hole 1210A (Cores 198-1210A-24H to 27H, where the hole terminates), 3 of which are interpreted as Danian (Samples 198-1210A-24H-4, 38 cm, 40 cm, and 44 cm), based on the presence of frequent and consistently occurring calcispheres and small foraminifer fragments. A total of 112 samples were examined from Hole 1210B (Cores 198-1210B-24H to 42H, where the hole terminates). Preservation is generally moderate and nannofossil abundance high throughout this relatively chert-free succession.

Tables **T6** and **T7** show the nannofossil distributions for these holes. Hole 1210A is upper Maastrichtian (Subzones UC20d<sup>TP</sup>–UC20b<sup>TP</sup>; CC26b–CC25c), whereas Hole 1210B is upper Maastrichtian–lower Campanian (Subzones UC20d<sup>TP</sup>–UC15b<sup>TP</sup>; CC26b–CC20). Hole 1210B contains the only succession that records the expected sequence of consecutive FOs of *L. quadratus* and *Micula murus* (bases of Subzones UC20a<sup>TP</sup> and UC20b<sup>TP</sup>, respectively) in Core 198-1210B-26H. However, the succession is similar to other sites of this age in that the bases of Zone UC19 (LO of *R. levis*) and Subzone UC15e<sup>TP</sup> (FO of *E. parallelus*) cannot be distinguished (see “**Discussion**,” p. 7). The uppermost Maastrichtian is present in Holes 1210A and 1210B, as illustrated by the presence of both *M. prinsii* and *C. ultimus*. The complete K/T boundary interval nannofossil data from this site are presented in Bown (in press).

Hole 1210B contains the MME between Sections 198-1210B-28H-5, 72 cm, and 28H-6, 52 cm (262.92–264.22 mbsf), with a further layer of inoceramid prisms at 261.48 mbsf (Frank et al., 2005). The LO of *Z. bicrescenticus* lies below the single layer of prisms but above the MME in-

---

**T4.** Range chart, Hole 1209A, p. 32.

---

---

**T5.** Range chart, Hole 1209C, p. 33.

---

---

**T6.** Range chart, Hole 1210A, p. 34.

---

---

**T7.** Range chart, Hole 1210B, p. 35.

---

terval proper. The MME lies above the LOs of *C. echinus* and *T. orionatus*, in the undifferentiated Zones UC18–UC19 (CC24–CC25a).

### Site 1211

A total of 22 smear slides were examined from Hole 1211A (Cores 198-1211A-15H to 18H, in which the hole terminates) and 5 from Hole 1211C (Core 198-1211C-15H, in which the hole terminates). In general, preservation was moderate and nannofossil abundance high throughout.

The nannofossil stratigraphic distributions are shown in Tables T8 and T9. Hole 1211A is uppermost Maastrichtian (Subzone UC20d<sup>TP</sup>) to upper–lower Maastrichtian (Subzone UC20a<sup>TP</sup>–Zone UC18; CC26b to CC25b–CC24), whereas Hole 1211C is uppermost Maastrichtian (Subzone UC20d<sup>TP</sup>; CC26b). The apparently reversed FOs of *M. murus* and *L. quadratus* in the Maastrichtian are discussed below, along with the absence of *R. levis*, which means that Zone UC18–Subzone UC20a<sup>TP</sup> (lower–upper Maastrichtian; Core 198-1211A-18H) cannot be differentiated (see “Discussion,” p. 7). The uppermost Maastrichtian is present in Hole 1211A, based on the presence of both *M. prinsii* and *C. ultimus*. The complete K/T boundary interval nannofossil data from this site are presented in Bown (in press).

Isolated inoceramid prisms are present in Section 198-1211A-18H-2 (~157.0 mbsf, from the original core descriptions in Bralower, Premoli Silva, Malone, et al., 2002), although Frank et al. (2005) do not consider these to be representative of the MME. However, these isolated prisms lie at/immediately above the LO of *Z. bicuspidatus* and above the LOs of *C. echinus* and *T. orionatus* in undifferentiated Zone UC18–Subzone UC20a<sup>TP</sup> (CC24–CC25b), as at previous sites.

### Site 1212

Two samples were analyzed from Hole 1212A (Cores 198-1212A-12H to 13H; flow-in was a problem below the samples analyzed from Section 13H-1, and coring terminated in this core) and 63 from Hole 1212B (Cores 198-1212B-11H to 25H, except for 16H, which had no recovery; the hole terminates in chert). Preservation and nannofossil abundance were generally moderate and high, respectively.

The nannofossil stratigraphic distributions are shown in Tables T10 and T11. The two samples from Hole 1212A were uppermost Maastrichtian (Subzone UC20d<sup>TP</sup>; CC26b). Hole 1212B contains the uppermost Maastrichtian (Subzone UC20d<sup>TP</sup>; CC26b) to the lower Cenomanian (Subzones UC2c–UC1b; in CC9c). The uppermost Maastrichtian is present in both holes, indicated by the presence of *M. prinsii*. *C. ultimus* was not present in the samples analyzed, however. The complete K/T nannofossil succession is presented in Bown (in press). The reversed FOs of *M. murus* and *L. quadratus* in the Maastrichtian and the absence/nonutility of a number of Maastrichtian (*R. levis*) and Campanian (*E. parallelus* and *Uniplanarius sissinghii*) marker species are discussed below. The oldest Campanian preserved here appears to lie above a mid-Campanian to lower Coniacian hiatus (Subzone UC15a<sup>TP</sup>–Zone UC10; CC19–CC14), as indicated by a concentration of FOs in Section 198-1212B-24H-6 between 1 and 30 cm. Below this, Subzones UC9a–UC9c could not be separated because of the sporadic occurrence of *Z. biperforatus* and/or the absence from the region of *B. parca expansa*. Another

---

T8. Range chart, Hole 1211A, p. 36.

---

---

T9. Range chart, Hole 1211C, p. 37.

---

---

T10. Range chart, Hole 1212A, p. 38.

---

---

T11. Range chart, Hole 1212B, p. 39.

---

hiatus was identified in Section 198-1212B-24H-6 between 30 and 30.5 cm, as indicated again by the concentration of FOs/LOs at 30.5 cm, effectively removing Subzones UC8b–UC3c (CC10b–CC13a; middle Turonian–upper Cenomanian). This condensed section resulted in the compression of Subzones UC3a–UC3b, rendering them indistinguishable from one another. Subzones UC2c–UC1b (lower Cenomanian) also could not be differentiated; some events were higher than expected (FOs of *Cylindralithus sculptus* and *Gartnerago segmentatum*) or lower than expected (FO of *Helicolithus anceps*) or the marker taxa were absent from this site (*Zeugrhabdotus xenotus*) or the region (*C. kennedyi* and *C. anfractus*).

Isolated inoceramid prisms were found in Sample 198-1212B-18H-1, 94–96 cm (144.64 mbsf, from initial core descriptions in Bralower, Premoli Silva, Malone, et al., 2002), although these were not considered to constitute the MME proper (Frank et al., 2005). The prism layer lies at/immediately above the LOs of *T. orionatus* and *C. echinus* but below the LO of *Z. bicrescenticus*. This is apparently older than at Site 1211, lying at the base of undifferentiated Zone UC18–Subzone UC20a<sup>TP</sup> (CC24–CC25b).

### Site 1213

Seven smear slides were analyzed from Core 198-1213A-7R; below this core, chert was predominant. The nannofloras were generally poorly preserved resulting in the loss of many taxa, although abundance was high. The stratigraphic distribution is shown in Table T12, but the ages assigned (upper–lower Campanian to lower Coniacian–lower Turonian; Subzones UC15e<sup>TP</sup>–UC15b<sup>TP</sup> to UC9c–UC8a; CC22c–CC20 to CC13b–CC12) are of very low resolution due to the loss of many marker taxa.

### Correlation between Sites

Figure F2 shows the correlation between the sites and gives an overview of the occurrence of chert in relation to the biostratigraphy.

## DISCUSSION

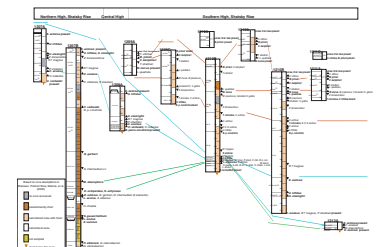
### Biostratigraphy

It can be seen from the stratigraphic charts (Tables T1–T12) and the correlation summary (Fig. F2) that certain taxa used in the most recent global Upper Cretaceous UC biozonation of Burnett (1998) were either absent or unreliable at Shatsky Rise or that certain intervals were either condensed or contained hiatuses, resulting in combination of biozones and reduced stratigraphic resolution. The low-resolution problem is particularly, and predictably, apparent in the Campanian, which is the interval of greatest nannofossil paleobiogeographic differentiation (e.g., Lees, 2002). The preponderance of condensed section was generally due to the lack of ooze material in chert intervals and was a problem restricted to the pre-Campanian.

In the upper Maastrichtian, the FOs of *M. murus* and *L. quadratus* appear to be reversed in Holes 1209C, 1211A, and 1212B but not in 1210B, although this latter effect may be a result of bioturbation (it should be noted that bioturbation was not recorded in the core descrip-

T12. Range chart, Hole 1213A, p. 40.

F2. Correlation of nannofossil (sub)zones, p. 28.



tion for Core 198-1210B-26H, although it may not have been apparent in these pure white oozes, and so this occurrence remains somewhat enigmatic) (Bralower, Premoli Silva, Malone, et al., 2002). This reversal means that the base of Subzone UC20a<sup>TP</sup> cannot be recognized. This appears to be a real signal since both taxa have consistent occurrences, species concepts were rigorously applied, and there are no deleterious changes in preservation to explain the possible loss of *L. quadratus* from lower samples. It is possible that *M. murus* has a diachronous FO; Self-Trail (2001) noted this phenomenon in the western Atlantic region, where *M. murus* was shown to occur first in a deep-ocean setting and later in a near-shore environment. However, this diachroneity occurred above the FO of *L. quadratus*. Further study is required to clarify this situation. For the time being, the FO of *M. murus* was used as the more reliable datum since this lower-latitude-preferring species was relatively more abundant and conspicuous in the studied sections.

Two previously unused biostratigraphic events were noted from the Shatsky Rise region that may prove to have utility across the Pacific in subdividing the upper Maastrichtian: the FO of *C. ultimus* in Subzone UC20d<sup>TP</sup> and the LO of *Tegumentum stradneri* in Subzone UC20b<sup>TP</sup> (see Fig. F2).

Lower in the Maastrichtian, Zones UC18 and UC19 could not be differentiated because the LO of *R. levis* could not be determined. This species, common in Subantarctic to Temperate Paleobiogeographic Zones (PBZs) in the Indian Ocean (Lees, 2002), is extremely rare and sporadic at Shatsky Rise, present only in Hole 1210B and questionably in Hole 1212B but absent from Holes 1209C and 1211A. Its distribution and utility is therefore definitely affected by biogeographic factors. It is possible that the biostratigraphic resolution (lost through the nonutility of both *R. levis* and *L. quadratus* in the lower Maastrichtian) could be supplemented by a number of events identified here, namely (in reverse stratigraphic order), the FOs of *Micula praemurus* and consistent *Cribrorona gallica*, the LOs of *Z. bicrescenticus* and *C. echinus*, and the FO of *C. echinus*.

Subzones UC15d<sup>TP</sup> and UC15e<sup>TP</sup> in the upper Campanian could not be differentiated because the marker species, *E. parallelus*, was either not present or could not be reliably determined at Shatsky Rise because the distinguishing crossbars that span the central area were missing from many eiffellithid specimens. The species is present in the region, occurring in Holes 1209A, 1209C, 1210A, 1210B, 1211A, and 1212B, but was recorded only sporadically and with its FO always occurring well above the expected stratigraphic level. It is probable that we have included specimens of this species without bars in *Eiffellithus turriseiffelii*, since *E. parallelus* was shown by Lees (2002) to be present in all PBZs in the Indian Ocean although, until further study is completed (Lees, unpubl. data), we cannot assume that the FO of *E. parallelus* is a reliable marker in the Pacific Ocean.

Some problems were experienced in reliably determining the FO of *U. sissinghii*, since this species seems to represent the end-member of a morphological continuum from *Uniplanarius gothicus* through specimens identified here as *Uniplanarius* cf. *U. sissinghii*. Consequently, in Hole 1212B, *U. sissinghii* apparently first occurs above the FO of *Uniplanarius trifidus*. In that instance, it is possible that we have included early forms of *U. sissinghii* with *U. gothicus* since in this hole we did not log intermediate forms.

The boundary between Subzones UC14d<sup>TP</sup> and UC15a<sup>TP</sup> could not be determined. According to Lees (2002, table 4), the marker species *M.*

*pleniporus* does not occur in the Tropical PBZ. Thus, this is the most likely reason for its absence from Shatsky Rise. Although *B. hayi* is possibly restricted to the Tropical PBZ (Lees, 2002, table 4), it also is not present at Shatsky Rise. Consequently, the base of Subzone UC14c<sup>TP</sup> cannot be recognized. This suggests that during the early Campanian Shatsky Rise lay in a situation at the biogeographic limits of these two species, possibly straddling the (Sub)tropical/Temperate PBZ divide (see “Biogeography,” p. 9, below).

The lack of high biostratigraphic resolution through the Campanian is possibly insurmountable in a global biozonation scheme due to the peak in nannofossil endemicity experienced at that time, but there are a number of biostratigraphic events that are useful in subdividing this interval on Shatsky Rise and that may have potential applicability to the wider Pacific region. These untested datums comprise the LO of *Rucinolithus? magnus* in Zone UC16, the FO of *R.? magnus* in Subzone UC15b<sup>TP</sup>, the FO of *Perchnielsenella stradneri* in Subzones UC15a<sup>TP</sup> or UC15b<sup>TP</sup>, and the FO of *Ceratolithoides indiensis* in undifferentiated Subzones UC14d<sup>TP</sup>–UC15d<sup>TP</sup>.

Note that we have declined to erect formal subzones using the proposed potential marker taxa listed above until further studies reveal their broad utility across the Pacific (Lees, unpubl. data).

### Biogeography

Work is in progress to determine Upper Cretaceous nannofossil paleobiogeography and consequent climate change for 5-m.y. time intervals in the wider Pacific region (Lees, unpubl. data). However, some preliminary broad paleobiogeographic inferences can be drawn for the Shatsky Rise sites using the deductions of Lees (2002, table 4) from Indian Ocean data and including a summary of the biogeographic observations from various oceans of numerous authors, most importantly Worsley (1974), Thierstein (1976, 1981), Roth (1978), Wind (1979), Roth and Bowdler (1981), Shafik (1990), Huber and Watkins (1992), Mutterlose (1992), Watkins et al. (1996), and Street and Bown (2000). It should be noted that a tropical to subtropical influence is expected, since the sites lay between 10°N and 20°N during the Late Cretaceous (Bralower, Premoli Silva, Malone, et al., 2002).

In the pre-Campanian Upper Cretaceous, the taxa that dominated assemblages at Sites 1207 and 1212 are mainly ones that Lees (2002, table 4) determined as dominant in the Austral to Temperate PBZs of the Indian Ocean. These include *Biscutum ellipticum* (abundant), *Biscutum* cf. *B. ellipticum*, *Discorhabdus ignotus*, *Manivitella pemmatoidea*, *Prediscosphaera columnata*, *Prediscosphaera ponticula*, and *Tetrapodorhabdus decorus* (all common). Common *Eiffellithus gorkae* was also found at Site 1212. Lees (2002) indicated that this was indicative of the Austral PBZ, although it is known to be dominant in Temperate sediments (J.M. Self-Trail, pers. comm., 2004); additionally, Lees (2002) lacked low-latitude data for this interval, so this indicator is likely misleading. It is important to note the absence of *Seribiscutum primitivum* and *Repagulum parvidentatum* from Shatsky Rise. *S. primitivum* was only recorded at temperate and austral latitudes in the Indian Ocean, even during times when tropical data were available, and is only ever abundant in the Austral PBZ (Lees, 2002, and others). *R. parvidentatum* is also only abundant in the Austral PBZ of the Indian Ocean but does have a rare record into the Tropical PBZ (Lees, 2002). Consequently, we can say that there was no austral (or boreal, since these taxa are bipolar) influence on

Shatsky Rise. Nannofossils indicative of a Tropical PBZ over Shatsky Rise include common *Rotelapillus crenulatus* at Site 1212 (conforming to Lees' deduction [Lees, 2002]) and common *Hayesites*, a genus that Street and Bown (2000) showed to have a low-latitude distribution, at Site 1207 (and all mid-Cretaceous sites). The absence of *Hayesites* from the Indian Ocean Temperate and Austral PBZs at this time is a major assemblage difference, and so it can be confirmed that Shatsky Rise was tropically situated in the pre-Campanian, but it may also have come under the occasional influence of cooler, temperate waters.

In the Campanian, for which there are low-latitude data from the Indian Ocean, although only from one site (Lees, 2002), there seems to be a mixture of tropical and temperate influences over Shatsky Rise. Note that *S. primitivum* and *R. parvidentatum* are again absent from Shatsky Rise, and so no austral influence is inferred. Tropical indicators include *Ceratolithoides brevicorniculans* and *U. sissinghii* (Lees, 2002). The former species occurs frequently to rarely at Sites 1210 and 1212 but is absent from Sites 1207 and 1208, whereas the latter occurs frequently to rarely at all sites. Intriguingly, *Lapideacassis asymmetrica* was noted as endemic in the Indian Ocean Temperate PBZ (Lees, 2002) but here is restricted to Sites 1210 and 1212, which occupy a more southerly position on Shatsky Rise. Common *Rotelapillus (Cylindralithus) biarcus*, used to define the early Campanian Temperate PBZ in the Indian Ocean (Lees, 2002), is only found at Site 1207; however, *L. grillii*, the common occurrence of which was also used to define the Temperate PBZ, is very poorly represented at all sites. Common *D. ignotus* and *Broinsonia parca constricta*, used to denote the Austral to Temperate PBZs in the Indian Ocean (Lees, 2002), were here found commonly only at the northerly Site 1207 in the Campanian. A number of other taxa noted as common in the Indian Ocean Austral to Temperate PBZs (Lees, 2002) occur commonly in most if not all of Sites 1207, 1208, 1212, and 1210 and include *Eiffelithus eximius*, *M. pemmatoidea*, *Microrhabdulus decoratus*, *Microrhabdulus undosus*, *P. ponticula*, *Prediscosphaera stoveri*, and *T. decorus*. This cursory and temporally broad examination of the nannofloras seems to suggest subtle paleobiogeographic differences emerging between the different sites on Shatsky Rise during the Campanian.

In the Maastrichtian, *S. primitivum* and *R. parvidentatum* are again absent, suggesting a lack of austral influence at Shatsky Rise. Commonly occurring Tropical PBZ indicators include *M. murus* (common at Sites 1209, 1210, and 1211), *Ceratolithoides pricei*, *Lithraphidites praequadratus*, *L. quadratus*, and *M. praemurus* (all present at Sites 1209, 1210, 1211, and 1212 but not common at any). *Ceratolithoides kamptneri* and *C. ultimus* were identified as endemic Tropical PBZ taxa by Lees (2002), and these occur at all sites of this age except for *C. ultimus*, which does not occur at Site 1212 (probably because the uppermost Maastrichtian was not examined). However, again there is some evidence of a temperate influence over Shatsky Rise, based on common occurrences of *Cylindralithus nudus*, *D. ignotus*, *M. decoratus*, *M. undosus*, *Placozygus fibuliformis*, *P. ponticula*, *P. stoveri*, and *T. decorus*. According to Lees (2002), a possible austral influence is, however, indicated by common *Corolithion? madagaskarensis* at Site 1210; *Retecapsa schizobrachiata* at Sites 1209, 1210, and 1211; and also possibly *Z. bicrescenticus* at Site 1212. However, *C.? madagaskarensis* and *Z. bicrescenticus* have apparently both been recorded commonly in temperate-subtropical assemblages (J.M. Self-Trail, pers. comm., 2004). Once again, there appear to be some distinct differences in the nannofloras between the sites.

Some taxa that are absent or occur rarely on Shatsky Rise and that are worthy of note include the holococcoliths, especially *Acuturris*, *Calculites obscurus*, and *Lucianorhabdus cayeuxii*. All of these genera have been found commonly to abundantly in both shelfal and oceanic situations in the Indian Ocean but had a preference for the Austral PBZ (Lees, 2002). However, they also occurred, albeit only rarely to frequently, down to the Tropical PBZ (Lees, 2002), so their absence from Shatsky Rise is enigmatic. *Nephrolithus*, which is a renowned high-latitude (sub-antarctic–austral/boreal) genus, is absent at Shatsky Rise, although it did reach down to the Tropical PBZ in the late Maastrichtian of the Atlantic (Self-Trail, 2001) and Indian Oceans (Lees, 2002). This may be further evidence that there was no high-latitude influence over Shatsky Rise in the Maastrichtian. Alternatively, since it is present in the low-latitude Atlantic and Indian Oceans, this may indicate unconformity at Shatsky Rise. *Reinhardtites*, with a preference for Austral to Temperate (*R. anthophorus*) and Subantarctic to Temperate (*R. levis*) PBZs in the Indian Ocean but with paleobiogeographic ranges down into the Tropical PBZ (Lees, 2002), occurred only rarely and very sporadically on Shatsky Rise. Similarly, *Gartnerago* and *Kamptnerius* had only rare and very sporadic distributions on Shatsky Rise; both preferred higher latitudes in the Indian Ocean (Lees, 2002). *M. pleniporus*, which only occurred down to the Temperate PBZ in the Indian Ocean (Lees, 2002), is missing from Shatsky Rise.

### **Mid-Maastrichtian Event**

As described above, the MME and layers of isolated inoceramid prisms (see Frank et al., 2005) occur around the level of the LO of *Z. bicuspidatus* in Holes 1209C, 1210B, 1211A, and 1212B, following the LOs of *C. echinus* and *T. orionatus*. There is currently no evidence to support a change in nannofloral productivity levels through this interval (Frank et al., 2005).

### **ACKNOWLEDGMENTS**

We are indebted to Tracy Frank for waiting patiently for data, to her and Mark Leckie for fruitful, frantic stratigraphic discussions, and to Mitch Malone for appreciating that these discussions take time! We are grateful to ODP for responding so rapidly to a belated request for supplementary samples. We sincerely thank David K. Watkins and Jean M. Self-Trail for their stimulating and encouraging reviews. Finally, J.A.L. would like to thank especially Tim Bralower and Paul Bown for allowing her to “muscle-in” on this project and associated meetings, despite not making it onto the ship! This research used samples and/or data provided by the Ocean Drilling Program (ODP). ODP is sponsored by the U.S. National Science Foundation (NSF) and participating countries under the management of the Joint Oceanographic Institutions (JOI), Inc. Funding for this research (J.A.L.) was received from NSF EAR-0318584, provided to Tim Bralower.

## REFERENCES

- Bown, P.R. (Ed.), 1998. *Calcareous Nannofossil Biostratigraphy*: Dordrecht, The Netherlands (Chapman-Hall).
- Bown, P.R., in press. Selective calcareous nannoplankton survivorship at the Cretaceous/Tertiary boundary. *Geology*.
- Bown, P.R., and Young, J.R., 1997. Mesozoic calcareous nannoplankton classification. *J. Nannoplankton Res.*, 19:21–36.
- Bown, P.R., and Young, J.R., 1998. Techniques. In Bown, P.R. (Ed.), *Calcareous Nannofossil Biostratigraphy*: Dordrecht, The Netherlands (Kluwer Academic Publ.), 16–28.
- Bralower, T.J., Premoli Silva, I., Malone, M.J., et al., 2002. *Proc. ODP, Init. Repts.*, 198 [CD-ROM]. Available from: Ocean Drilling Program, Texas A&M University, College Station TX 77845-9547, USA.
- Bukry, D., 1969. Upper Cretaceous coccoliths from Texas and Europe. *Univ. Kansas Paleontol. Contrib.*, Article 51 (Protista 2), 1–79.
- Bukry, D., 1973. Phytoplankton stratigraphy, Deep Sea Drilling Project Leg 20, western Pacific Ocean. In Heezen, B.C., MacGregor, I.D., et al., *Init. Repts. DSDP*, 20: Washington (U.S. Govt. Printing Office), 307–317.
- Bukry, D., 1975. Coccolith and silicoflagellate stratigraphy, northwestern Pacific Ocean. In Larsen, R.L., Moberly, R., et al., *Init. Repts. DSDP*, 32: Washington (U.S. Govt. Printing Office), 677–701.
- Burnett, J.A., 1997. New species and conjectured evolutionary trends of *Ceratolithoides* from the Campanian and Maastrichtian of the Indian Ocean. *J. Nannoplankton Res.*, 19(2):123–131.
- Burnett, J.A., with contributions from Gallagher, L.T., and Hampton, M.J., 1998. Upper Cretaceous. In Bown, P.R. (Ed.), *Calcareous Nannofossil Biostratigraphy*: Dordrecht, The Netherlands (Kluwer Academic Publ.), 132–199.
- Frank, T.D., Thomas, D.J., Leckie, R.M., Arthur, M.A., Bown, P.R., Jones, K., and Lees, J.A., 2005. The Maastrichtian record from Shatsky Rise (northwest Pacific): a tropical perspective on global ecological and oceanographic changes. *Paleoceanography*, 20(1):PA1008.
- Hattner, J.G., and Wise, S.W., 1980. Upper Cretaceous calcareous nannofossil biostratigraphy of South Carolina. *S. C. Geol.*, 24:41–117.
- Holmes, M.A., and Watkins, D.K., 1992. Middle and Late Cretaceous history of the Indian Ocean. In *Synthesis of Results from Scientific Drilling in the Indian Ocean*. Geophys. Monogr., 70:225–244.
- Huber, B.T., and Watkins, D.K., 1992. Biogeography of Campanian–Maastrichtian calcareous plankton in the region of the Southern Ocean: paleogeographic and paleoclimatic implications. In *The Antarctic Paleoenvironment: A Perspective on Global Change*. Antarc. Res. Ser., 56:31–60.
- Kennedy, W.J., Gale, A.S., Bown, P.R., Caron, M., Davey, R.J., Gröcke, D., and Wray, D.S., 2000. Integrated stratigraphy across the Aptian–Albian boundary in the Marne Bleues, at the Col de Pré-Guiterd, Arnayon (Drôme), and at Tortonne (Alpes-de-Haute-Provence), France: a candidate global boundary stratotype section and boundary point for the base of the Albian Stage. *Cretaceous Res.*, 223:591–720.
- Klaus, A., and Sager, W.W., 2002. Data report: High-resolution site survey seismic reflection data for ODP Leg 198 drilling on Shatsky Rise, northwest Pacific. In Bralower, T.J., Premoli Silva, I., Malone, M.J., et al., *Proc. ODP, Init. Repts.*, 198, 1–21 [CD-ROM]. Available from: Ocean Drilling Program, Texas A&M University, College Station TX 77845-9547, USA.
- Lees, J.A., 2002. Calcareous nannofossil biogeography illustrates palaeoclimate change in the Late Cretaceous Indian Ocean. *Cretaceous Res.*, 23:537–634.
- Mutterlose, J., 1992. Biostratigraphy and palaeobiogeography of Early Cretaceous calcareous nannofossils. *Cretaceous Res.*, 13:157–189.

- Perch-Nielsen, K., 1979. Calcareous nannofossils from the Cretaceous between the North Sea and the Mediterranean. *In* Wiedmann, J. (Ed.), *Aspekte der Kreide Europas*. Int. Union Geol. Sci. Ser. A, 6:223–272.
- Perch-Nielsen, K., 1983. Recognition of Cretaceous stage boundaries by means of calcareous nannofossils. *In* Birkelund, T., Bromley, R., Christensen, W.K., Håkansson, E., and Surlyk, F. (Eds.), *Symposium on Cretaceous Stage Boundaries, Copenhagen*, 152–156. (Abstract)
- Perch-Nielsen, K., 1985. Mesozoic calcareous nannofossils. *In* Bolli, H.M., Saunders, J.B., and Perch-Nielsen, K. (Eds.), *Plankton Stratigraphy*: Cambridge (Cambridge Univ. Press), 329–426.
- Robinson, S.A., Williams, T., and Bown, P.R., 2004. Fluctuations in biosiliceous production and the generation of Early Cretaceous oceanic anoxic events in the Pacific Ocean (Shatsky Rise, Ocean Drilling Program Leg 198). *Paleoceanography*, 19:PA4024.
- Roth, P.H., 1973. Calcareous nannofossils. *In* Winterer, E.L., Ewing, J.I., et al., *Init. Repts. DSDP*, 17: Washington (U.S. Govt. Printing Office), 695–795.
- Roth, P.H., 1978. Cretaceous nannoplankton biostratigraphy and oceanography of the northwestern Atlantic Ocean. *In* Benson, W.E., Sheridan, R.E., et al., *Init. Repts. DSDP*, 44: Washington (U.S. Govt. Printing Office), 731–759.
- Roth, P.H., and Bowdler, J., 1981. Middle Cretaceous calcareous nannoplankton biogeography and oceanography of the Atlantic Ocean. *In* Warme, J.E., Douglas, R.G., and Winterer, E.L. (Eds.), *The Deep Sea Drilling Project: a Decade of Progress*. Spec. Publ.—Soc. Econ. Paleontol. Mineral., 32:517–546.
- Self-Trail, J.M., 2001. Biostratigraphic subdivision and correlation of upper Maastrichtian sediments from the Atlantic Coastal Plain and Blake Nose, western Atlantic. *In* Kroon, D., Norris, R.D., and Klaus, A. (Eds.), *Western North Atlantic Paleogene and Cretaceous Paleoceanography*, Spec. Publ.—Geol. Soc. London, 183:93–110.
- Shafik, S., 1990. Late Cretaceous nannofossil biostratigraphy and biogeography of the Australian western margin. *Bull.—Bur. Min. Resour. Geol. Geophys. Aust.*, 295:1–164.
- Sissingh, W., 1977. Biostratigraphy of Cretaceous calcareous nannoplankton. *Geol. Mijnbouw*, 56:37–65.
- Sissingh, W., 1978. Microfossil biostratigraphy and stage-stratotypes of the Cretaceous. *Geol. Mijnbouw*, 57:433–440.
- Street, C., and Bown, P.R., 2000. Palaeobiogeography of Early Cretaceous (Berriasian–Barremian) calcareous nannoplankton. *Mar. Micropaleontol.*, 39:265–291.
- Thierstein, H.R., 1976. Mesozoic calcareous nannoplankton biostratigraphy of marine sediments. *Mar. Micropaleontol.*, 1:325–362.
- Thierstein, H.R., 1981. Late Cretaceous nannoplankton and the change at the Cretaceous–Tertiary boundary. *In* Warme, J.E., Douglas, R.G., and Winterer, E.L. (Eds.), *The Deep Sea Drilling Project: A Decade of Progress*. Spec. Publ.—Soc. Econ. Paleontol. Mineral., 32:355–394.
- Tremolada, F., and Erba, E., 2002. Morphometric analysis of Aptian *Assipetra infracretacea* and *Rucinolithus terebrodentarius* nannoliths: implications for taxonomy, biostratigraphy and paleoceanography. *Mar. Micropaleontol.*, 44:77–92.
- Varol, O., 1992. Taxonomic revision of the Polycyclolithaceae and its contribution to Cretaceous biostratigraphy. *Newsl. Stratigr.*, 27:93–127.
- Watkins, D.K., Wise, S.W., Jr., Pospichal, J.J., and Crux, J., 1996. Upper Cretaceous calcareous nannofossil biostratigraphy and paleoceanography of the Southern Ocean. *In* Mognilevsky, A., and Whatley, R. (Eds.), *Microfossils and Oceanic Environments*: Univ. of Wales (Aberystwyth Press), 355–381.
- Wind, F.H., 1979. Maestrichtian–Campanian nannofloral provinces of the southern Atlantic and Indian Oceans. *In* Talwani, M., Hay, W., and Ryan, W.B.F. (Eds.), *Deep Sea Drilling Results in the Atlantic Ocean: Continental Margins and Paleoenvironment*. Am. Geophys. Union, Maurice Ewing Ser., 3:123–137.

- Worsley, T.R., 1974. The Cretaceous/Tertiary boundary event in the ocean. *In* Hay, W.W. (Ed.), *Studies in Paleo-oceanography*, Spec. Publ.—Soc. Econ. Paleontol. Mineral., 20:94–125.
- Young, J.R., Bergen, J.A., Bown, P.R., Burnett, J.A., Fiorentino, A., Jordan, R.W., Kleijne, A., van Niel, B.E., Ton Romein, A.J., and von Salis, K., 1997. Guidelines for coccolith and calcareous nannofossil terminology. *Paleontology*, 40:875–912.

## APPENDIX A

### Systematic Paleontology

The systematic paleontology section includes taxonomic discussion of key taxa and the description of seven new species (*Ahmuellerella alboradiata*, *Ceratolithoides perangustus*, *Ceratolithoides sagittatus*, *Tegumentum lucidum*, *Micula clypeata*, *Micula premolisilvae*, and *Uniplanarius clarkei*) and two new combinations (*Loxolithus thiersteinii* and *Rotelapillus biarcus*). The taxonomy follows the classification and organization of Bown and Young (1997) and Burnett (1998). Only bibliographic references not included in Perch-Nielsen (1985) and Bown (1998) are included in the reference list. A full taxonomic list of species cited in this paper follows below (see “Appendix B,” p. 22). Descriptive terminology follows the guidelines of Young et al. (1997), and the following abbreviations are used in taxonomic descriptions: LM = light microscope, XPL = cross-polarized light, and PC = phase-contrast illumination. Holotype dimensions are given in parentheses. The taxa are illustrated in Plates P1–P10. The scale bar on the first figure of each plate applies to all figures on that plate.

Family Chialstozygaceae Rood et al., 1973, emend. Varol and Girgis, 1994

*Ahmuellerella alboradiata* sp. nov.

Pl. P1, figs. 1–12

**Derivation of name:** From *albus*, meaning white, and *radiatus*, meaning with rays, referring to the distinctive XPL image of the central area plate of this coccolith.

**Diagnosis:** Medium-sized murolith coccolith with a narrow, unicyclic rim and a wide central area filled with a variably birefringent plate. The rim is dark under XPL. The central area plate is characterized by eight radial segments of alternating bright and dark birefringence, divided by axial and diagonal sutures. The center portion of the central plate appears to show narrow, near-axial cross bars that bear a short, broad spine (Pl. P1, fig. 3). The bars do not appear to extend to the rim.

**Differentiation:** The LM image is similar to *Ahmuellerella regularis* but is distinguished by the alternating birefringence of the central area plate (see Pl. P1, figs. 13–19).

**Dimensions:** length = 6.5–7.2 (6.6)  $\mu\text{m}$ ; width = 4.7–5.5 (5.0)  $\mu\text{m}$ .

**Holotype:** Pl. P1, fig. 1 (figs. 1–6 are the same specimen).

**Paratype:** Pl. P1, fig. 11 (figs. 10–12 are the same specimen).

**Type locality:** Hole 1209C, Shatsky Rise, northwest Pacific Ocean.

**Type level:** upper Maastrichtian, Sample 198-1209C-16H-6, 50 cm (Subzone UC20b<sup>TP</sup>).

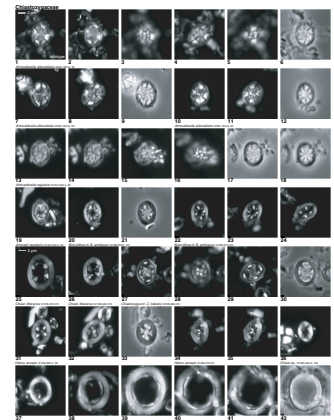
**Range:** upper Maastrichtian (Subzones UC20b<sup>TP</sup>–?UC20c<sup>TP</sup>); Sites 1209, ?1210.

*Chialstozygus* sp. with indistinct subaxial bars

Pl. P1, fig. 36

**Remarks:** Small loxolith with a broad rim and narrow central area; diagonal cross bars are occasionally visible in the central area.

P1. Chialstozygaceae, p. 41.



*Chiastozygus* cf. *C. trabalis* (Górka, 1957) Burnett, 1997a  
Pl. P1, figs. 27–30

**Remarks:** Similar to *Chiastozygus trabalis* but has brighter, more robust central area cross bars.

*Loxolithus thiersteinii* (Roth, 1973) comb. nov.  
Pl. P1, figs. 38–42

**Basionym:** *Crepidolithus thiersteinii* Roth, 1973, p. 725, pl. 22, fig. 6.

**Remarks:** Although both *Crepidolithus* and *Loxolithus* have elliptical, loxolith rims, the central area in *Loxolithus* is wide and open, whereas *Crepidolithus* typically has a narrow to closed central area. *Crepidolithus* is restricted to the Jurassic.

*Zeugrhabdotus embergeri* (Noël, 1958) Perch-Nielsen, 1984  
Pl. P2, figs. 19–20

*Zeugrhabdotus* cf. *Z. embergeri* (Noël, 1958) Perch-Nielsen, 1984  
Pl. P2, figs. 21–23

**Remarks:** Large, bicyclic loxolith coccoliths with an open central area spanned by a broad transverse bar. Specimens often display distinctive orange birefringence under XPL and were rather ragged in appearance, and thus distinguishable from more typical *Zeugrhabdotus embergeri* specimens. These specimens are noted as *Zeugrhabdotus* cf. *Z. embergeri* on the range charts but may conform to the species concept of *Zeugrhabdotus pseudanthophorus*. Alternatively, these specimens may simply be preservational morphotypes of *Zeugrhabdotus embergeri*.

Family Eiffellithaceae Reinhardt, 1965

*Tegumentum lucidum* sp. nov.  
Pl. P2, figs. 24–30

**Derivation of name:** From *lucidus*, meaning bright, referring to the distinctive bright XPL image of this coccolith.

**Diagnosis:** Medium-sized, murolith coccolith with a broad, bicyclic rim, dominated by the thick, bright inner-cycle and a narrow central area almost filled by short, broad, bright diagonal cross bars.

**Remarks:** The rim of this coccolith is highly distinctive, having a broad, bright (white) inner cycle and a very narrow, dark outer cycle. The LM appearance is most reminiscent of *Tegumentum* but is also similar to *Eiffellithus*. The broad, rounded, diagonal cross bars almost fill the narrow central area and are of similar birefringence to the inner rim cycle.

**Differentiation:** Differentiated from other species of *Tegumentum* by its narrower central area and broad rounded cross bars. Somewhat similar to the Early Cretaceous *Eiffellithus windii*, but the cross bar morphology is distinct and outer rim cycle narrower.

**Dimensions:** length = 5.0–6.5 (6.0)  $\mu\text{m}$ ; width = 3.5–5.0 (4.3)  $\mu\text{m}$ .

**Holotype:** Pl. P2, fig. 29 (figs. 29–30 are the same specimen).

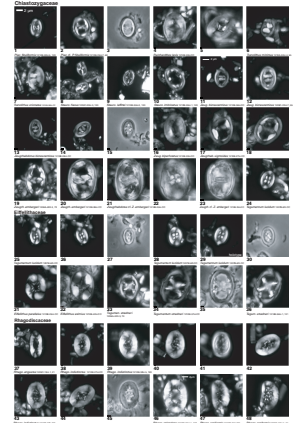
**Paratype:** Pl. P2, fig. 25 (figs. 25–27 are the same specimen).

**Type locality:** Hole 1207B, Shatsky Rise, northwest Pacific Ocean.

**Type level:** lower Campanian, Sample 198-1207B-6R-CC (Subzones UC14d<sup>TP</sup>–UC15a<sup>TP</sup>).

**Range:** lower Campanian–upper Maastrichtian (Subzones UC14d<sup>TP</sup>–UC15a<sup>TP</sup> to UC20d<sup>TP</sup>); Sites 1207, 1210, and 1212.

P2. Chiastozygaceae, Eiffellithaceae, Rhagodiscaceae, p. 43.



Family Stephanolithiaceae Black, 1968

*Rotelapillus biarcus* (Bukry, 1969) comb. nov.

Pl. P3, figs. 1–6

**Basionym:** *Cylindralithus biarcus* Bukry, 1969, p. 42, pl. 20, fig. 2.

**Remarks:** This species has comparable rim structure to other *Rotelapillus* coccoliths, but differs in having only two, rather than four, central area cross bars. *Cylindralithus* coccoliths have distinctly different rim structure, modified from the placolith *Watznaueria* group, and no central area bars. *Stoverius* has a low rim, whereas that of *Rotelapillus* is high.

Family Watznaueriaceae Rood et al., 1971

*Perchnielsenella stradneri* (Perch-Nielsen, 1973) Watkins  
in Watkins and Bowdler, 1984

Pl. P4, figs. 22–30

**Remarks:** A large, distinctive, highly birefringent coccolith, seen in both side and plan view. Observed commonly and consistently through the Campanian and Maastrichtian sediments from Shatsky Rise. The rim morphology most closely resembles *Cylindralithus*, to which it is most likely closely related.

**Dimensions:** length = 6.5–10.0 µm; height = 6.0–10.0 µm.

Heterococcoliths of uncertain affinity

*Cribracorona gallica* (Stradner, 1963) Perch-Nielsen, 1973

Pl. P4, figs. 42–48

**Remarks:** Distinctive circular to subcircular coccoliths seen in both side and plan view. Comparable in LM appearance to *Cylindralithus* but less birefringent in plan view and the two “shields” are clearly visible at different focal depths (see Pl. P4, figs. 44, 45). Additionally, the central area grille is very distinctive in *Cribracorona*. In side view the two genera are clearly distinguishable.

*Cribracorona echinus* (Bukry, 1975) comb. nov.

**Synonym:** *Petrobrasiella? bownii* Burnett, 1997a (Pl. P4, figs. 31–41).

**Basionym:** *Cylindralithus echinus* Bukry, 1975, p. 689, pl. 3, figs. 4, 5.

**Remarks:** Distinctive, stratigraphically short-ranging coccolith seen in both side and plan view. Originally described from Shatsky Rise, it is commonly present in the lower Maastrichtian Zone UC17 Sites 1210 and 1212.

**Dimensions:** length = 6.5–7.0 µm; height = ~6.0 µm.

Nannoliths

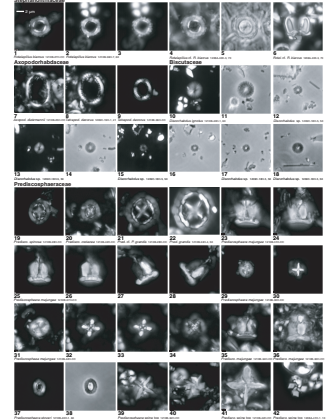
*Assipetra terebrodentarius* (Applegate et al. in Covington and Wise, 1987)  
Rutledge and Bergen in Bergen, 1994

Pl. P5, figs. 19–21

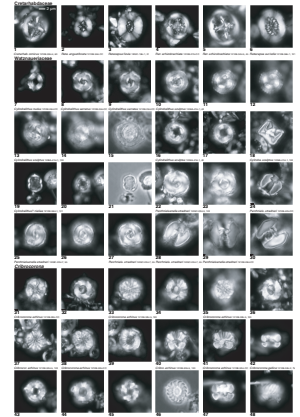
**Description:** Blocky globular nannoliths formed from six or more complexly intergrown calcite blocks that are joined along broadly radial sutures; roughly circular in plan and rectangular in side view.

**Remarks:** *Assipetra terebrodentarius* has rarely been reported from Upper Cretaceous sediments, but it is consistently present in the Aptian–Campanian of the Shatsky Rise sites, with a probable last occurrence in the upper Campanian. The forms observed are usually the larger morphotype, *A. terebrodentarius youngii* (Tremolada and Erba, 2002; >8.0 µm; see Bown, this volume). Tremolada and Erba (2002) considered this subspecies to be restricted in stratigraphic

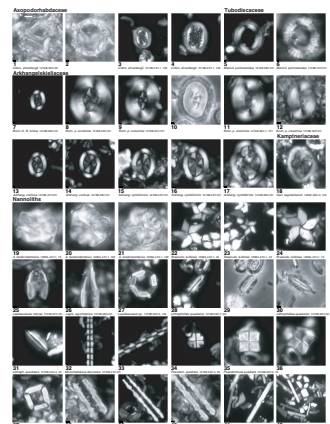
P3. Stephanolithiaceae, Axopodorhabdaceae, Biscutaceae, Prediscosphaeraceae, p. 45.



P4. Cretarhabdaceae, Watznaueriaceae, *Cribracorona*, p. 47.



P5. Axopodorhabdaceae, Tubodiscaceae, Arkhangelskiellaceae, Kampneriaceae, Nannoliths, p. 49.



range to the Aptian and possibly associated with unusual paleoceanographic conditions related to OAE1a and its immediate aftermath. We are uncertain of its paleoecology, but its presence in Upper Cretaceous sediments is without doubt, having also been observed in Upper Cretaceous sediments from the Indian Ocean (P.R. Bown, pers. observ.).

Genus *Ceratolithoides* Bramlette and Martini, 1964

**Remarks:** Arrowhead-shaped nannoliths constructed from two basal rectangular to rhombic elements and a narrow, apical, conical structure (Burnett, 1997). Morphological terminology employed below after Burnett (1997).

*Ceratolithoides perangustus* sp. nov.

Pl. P6, figs. 21–23

**Derivation of name:** From *perangustus*, meaning very narrow, referring to the shape of this nannolith.

**Diagnosis:** Small *Ceratolithoides* with tall, narrow base and narrow apical cone that does not protrude far above the base. The interhorn angle is usually between 90° and 180°, and there is no distinct shoulder.

**Differentiation:** Narrower morphology than other *Ceratolithoides* species.

**Dimensions:** length = (4.8) µm; width = (2.0) µm.

**Holotype:** Pl. P6, fig. 22 (figs. 22 and 23 are the same specimen).

**Paratype:** Pl. P6, fig. 21.

**Type locality:** Hole 1210B, Shatsky Rise, northwest Pacific Ocean.

**Type level:** upper Campanian, Sample 198-1210B-36H-7, 60 cm (Zone UC16).

**Range:** lower/upper to upper Campanian (Subzone UC15c<sup>TP</sup>–Zone UC16); Sites 1207 and 1210.

*Ceratolithoides sagittatus* sp. nov.

Pl. P6, figs. 25–30

**Derivation of name:** From *sagitta*, meaning arrow-shaped, referring to the shape of this nannolith.

**Diagnosis:** Small *Ceratolithoides* with rhombic basal elements and distinct, two-part apical cone. The cone protrudes significantly above the basal elements. The interhorn angle is usually just >90°.

**Differentiation:** The apical cone structure is highly distinctive, formed from two large elements, protruding significantly above the base, and not enclosed within the base.

**Dimensions:** length = 3.5–5.5 µm; width = 3.0–5.0 µm.

**Holotype:** Pl. P6, fig. 26.

**Paratype:** Pl. P6, fig. 27.

**Type locality:** Hole 1210B, Shatsky Rise, northwest Pacific Ocean.

**Type level:** upper Campanian, Sample 198-1210B-38H-CC (Subzones UC15d<sup>TP</sup>–UC15e<sup>TP</sup>).

**Range:** lower Campanian to upper Maastrichtian (Subzones UC15b<sup>TP</sup>–UC20b<sup>TP</sup>); Sites 1207, 1208, 1209, 1210, and 1212.

Family Polycyclolithaceae Forchheimer, 1972, emend. Varol, 1992

Genus *Micula* Vekshina, 1959

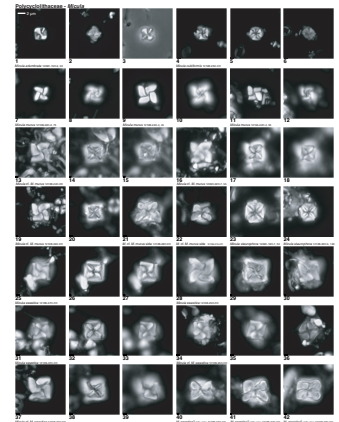
Pls. P7, P8

**Remarks:** Typically cubiform nannoliths usually formed from two superimposed and complexly intergrown cycles of four pyramidal/blocky elements each; one of the cycles may be reduced (*M. murus*), relict (*M. prinsii*), or lost (*M. clypeata*, *M. premolisilvae*, and *M. praemurus*). The elements are usually broadly triangular in shape and point/twist consistently in one direction on each surface; the elements may protrude slightly away from the edges of the cube.

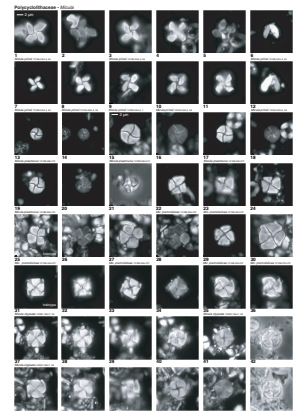
P6. *Ceratolithoides*, p. 51.



P7. Polycyclolithaceae–*Micula*, p. 53.



P8. Polycyclolithaceae II–*Micula*, p. 55.



When focusing through the structure in LM, the two cycles twist in opposite directions and, at mid-focus, the bright, diagonal, barlike structures typical of *Micula* are seen. All elements are bright under XPL when the sides of the cube/square are parallel with the polarizing directions, but the whole structure goes into extinction when rotated 45° from this position.

The morphology of *Micula* may be quite altered by overgrowth, and species often show intraspecific variation, exacerbated by their complex three-dimensional structure. The dominant *Micula* in the Campanian and Maastrichtian sediments at Shatsky Rise is *M. swastica*, although *M. murus* and *M. prinsii* become common in the uppermost Maastrichtian.

*Micula clypeata* sp. nov.

Pl. P8, figs. 31–48

**Derivation of name:** From *clypeus*, meaning “like a round shield,” referring to the shape of this nannolith.

**Diagnosis:** Square, flat *Micula* that appears to be composed of a single cycle of four elements joined along uneven sutures that bend sharply at their ends. A distinctive raised circular area, equal in diameter to the width of the nannolith, lies above the level of the main structure. A narrow zone of darker birefringence lies along each of the suture lines and broadens toward the corners.

**Differentiation:** Much flatter than most other *Micula* species but with the same crystallographic orientation (i.e., the entire structure is in extinction when the sutures are near-parallel with the polarizing directions). Similar to *M. praemurus*, particularly at high focus, but differs in having a square “base” and more complex suture appearance.

**Dimensions:** length/width = 5.5–6.5 (5.5) µm.

**Holotype:** Pl. P8, fig. 31 (figs. 31–34 are the same specimen).

**Paratype:** Pl. P8, fig. 37 (figs. 37–42 are the same specimen).

**Type locality:** Hole 1209C, Shatsky Rise, northwest Pacific Ocean.

**Type level:** upper Maastrichtian, Sample 198-1209C-18H-7, 50 cm (Subzone UC20b<sup>TP</sup>).

**Range:** lower Campanian?–upper Maastrichtian (Subzones UC15b<sup>TP</sup>–UC20d<sup>TP</sup>); Sites 1208, 1209, 1210, 1211, and 1212.

*Micula murus* (Martini, 1961) Bukry, 1973

Pl. P7, figs. 7–22

**Remarks:** *Micula* composed of two superimposed and complexly intergrown cycles, one much reduced in size, and each cycle twisting in opposite directions. In “normal view” the elements are broadly triangular in shape and point/twist consistently in one direction; the elements protrude significantly away from the edges of the cube. Side views of *M. murus* are thinner than the normal view and clearly show the two superimposed, differently sized cycles.

*Micula premolisilvae* sp. nov.

Pl. P8, figs. 22–30

**Derivation of name:** Named for Isabella Premoli Silva, micropaleontologist and ODP Leg 198 Co-Chief Scientist.

**Diagnosis:** A near-square to cruciform, flat *Micula*, composed of a single cycle of four elements joined along distinct straight, or gently curving, sutures.

**Differentiation:** Similar in morphology to *M. praemurus* but the outline is square or cruciform rather than circular. The orientation of the sutures is variable in the specimens observed, ranging from axial (Pl. P8, figs. 25–28) to near-diagonal (Pl. P8, figs. 22–24, 29, 30). Much flatter than other *Miculas*, *M. premolisilvae* is most similar to *M. praemurus* and *M. clypeata*, to which it may be more closely related. The entire nannolith goes into extinction when the sides of the square are rotated to 45° from the polarizing directions (Pl. P8, fig. 26).

**Dimensions:** length/width = 5.0–6.5 µm.

**Holotype:** Pl. P8, fig. 25 (figs. 25 and 26 are the same specimen).

**Paratype:** Pl. P8, fig. 27 (figs. 27 and 28 are the same specimen).

**Type locality:** Hole 1210B, Shatsky Rise, northwest Pacific Ocean.

**Type level:** upper Campanian, Sample 198-1210B-32H-CC (Zone UC16).

**Range:** upper Campanian–lower/upper Maastrichtian (Zones UC16 to UC1–UC19); Sites 1209, 1210, and 1212.

***Micula swastica* Stradner and Steinmetz, 1984**

Pl. P7, figs. 25–42

**Remarks:** *Micula* composed of two equidimensional, superimposed, and complexly intergrown cycles. In “normal view” the elements are broadly triangular in shape and point/twist consistently in one direction on each surface; the elements may protrude slightly beyond the cube. When focusing through the structure in LM, the two cycles twist in opposite directions and, at mid-focus, the bright diagonal image that typifies *Micula* is seen (Pl. P7, fig. 26). Side views of *M. swastica* are thinner than the normal view and clearly show the two superimposed cycles (Pl. P7, figs. 40–42).

Most likely, *M. swastica* gave rise to *M. murus* through reduction of one of the cycles, and intermediate morphologies render the FO of *M. murus* difficult to precisely identify. However, in this study, we were very careful in our application of the concept of *M. murus*, and, since the datum ties in well with the planktonic foraminifer biostratigraphy, we have high confidence in that datum.

***Micula praemurus* (Bukry, 1973) Stradner and Steinmetz, 1984**

Pl. P8, figs. 13–21

**Remarks:** A highly distinctive, circular, disklike *Micula*, originally described from Shatsky Rise (Bukry, 1973), composed of a single cycle of four elements joined along curving, S-shaped sutures. Much flatter than other *Miculas* but with comparable crystallographic orientation.

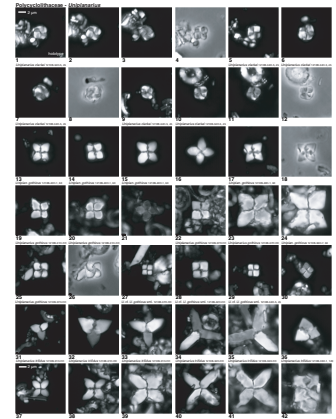
*Micula clypeata* and *Micula premolisilvae* share a number of morphological features that distinguish them from other *Micula* species and likely represent closely related forms. Despite the name, *Micula praemurus* does not appear a likely candidate for the direct ancestor of *Micula murus* (see *Micula swastica*).

***Uniplanarius* Hattner and Wise, 1980**

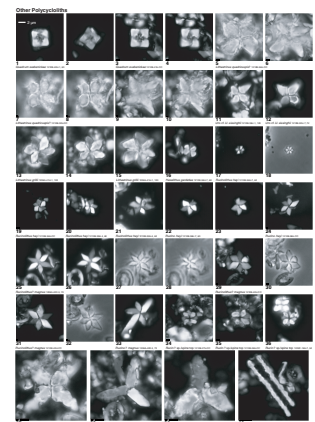
Pl. P9, P10

**Remarks:** Genus erected by Hattner and Wise (1980) for planar, radial nannoliths composed of three or four elements. We follow this concept and include the species *Uniplanarius gothicus*, *Uniplanarius trifidus*, *Uniplanarius sissinghii*, and a new species, *Uniplanarius clarkei*. We have not observed the two superimposed cycles or median diaphragm that Varol (1992) used to distinguish this genus from *Quadrum*. However, unlike Hattner and Wise (1980), we have retained use of the genus *Quadrum* for cubiform nannoliths typically formed from two superimposed cycles of four elements, each joined along straight, axial sutures (*Quadrum gartneri*). The transitional species, *Quadrum intermedium*, has additional, small elements inserted between the four major ones in one or both cycles. Using this definition, *Quadrum* is restricted to the upper Cenomanian–upper Coniacian. We believe the additional species *Quadrum eptabrachium*, *Quadrum octobrachium*, *Quadrum eneabrachium*, and *Quadrum giganteum*, described by Varol (1992), are *Eprolithus* specimens that have been modified by preservation.

**P9. Polycyclolithaceae III–*Uniplanarius*, p. 57.**



**P10. Other polycycloliths, p. 59.**



*Uniplanarius gothicus* (Deflandre, 1959) Hattner and Wise, 1980  
Pl. **P9**, figs. 13–24

*Uniplanarius* cf. *U. gothicus* (Deflandre, 1959) Hattner and Wise, 1980  
(small form)  
Pl. **P9**, figs. 27–30

**Remarks:** Small, square, simply constructed *Uniplanarius*. The elements are bright under XPL when the sutures and sides of the square nannolith are parallel to the polarizing directions and all in extinction when rotated to 45°. Similar in appearance to *Quadrum gartneri*, but the latter is blocky, cubiform, and constructed from two superimposed cycles of elements.

*Uniplanarius* cf. *U. sissinghii* (Deflandre, 1959) Hattner and Wise, 1980  
Pl. **P9**, figs. 37, 38

**Remarks:** *Uniplanarius* nannoliths that have longer free rays than typical specimens of *U. gothicus*, but not as long as those seen in *Uniplanarius sissinghii*.

*Uniplanarius clarkei* sp. nov.  
Pl. **P9**, figs. 1–12

**Derivation of name:** Named for Leon Clarke, paleoceanographer and ODP Leg 198 Shipboard Scientist.

**Diagnosis:** Small, square *Uniplanarius* with rounded corners, formed from four blocks joined along axial sutures that are marked under XPL by relatively broad zones of darker birefringence, together resembling the blades of a propeller. The outer edges of the nannolith may show slightly higher birefringence.

**Dimensions:** length/width = 3.3–4.0 (3.3)  $\mu\text{m}$ .

**Holotype:** Pl. **P9**, fig. 1 (figs. 1–4 are the same specimen).

**Paratype:** Pl. **P9**, fig. 10 (figs. 10–12 are the same specimen).

**Type locality:** Hole 1210B, Shatsky Rise, northwest Pacific Ocean.

**Type level:** upper Campanian, Sample 198-1210B-34H-5, 45 cm (Zone UC16).

**Range:** lower Campanian–uppermost Maastrichtian (Subzones UC14d<sup>TP</sup>–UC15a<sup>TP</sup> to UC20d<sup>TP</sup>); Sites 1207, 1208, 1209, 1210, 1211, and 1212.

## APPENDIX B

### Taxonomic List

A full list of all taxa cited in the text, figures, and range charts is given below. Most bibliographic references can be found in Perch-Nielsen (1985) and Bown (1998). Those that are not appear in the reference list herein.

- Ahmuellerella alboradiata* sp. nov.  
*Ahmuellerella octoradiata* (Górka, 1957) Reinhardt, 1966  
*Ahmuellerella regularis* (Górka, 1957) Reinhardt and Górka, 1967  
*Amphizygus brooksii* Bukry, 1969  
*Amphizygus minimus* Bukry, 1969  
*Arkhangelskiella confusa* Burnett, 1997a  
*Arkhangelskiella cymbiformis* Vekshina, 1959  
*Arkhangelskiella maastrichtiana* Burnett, 1997a  
*Assipetra terebrodentarius* (Applegate et al. in Covington and Wise, 1987) Rutledge and Bergen in Bergen, 1994  
*Axopodorhabdus albianus* (Black, 1967) Wind and Wise in Wise and Wind, 1977  
*Axopodorhabdus dietzmannii* (Reinhardt, 1965) Wind and Wise, 1983  
*Biantholithus sparsus* Bramlette and Martini, 1964  
*Biscutum* Black in Black and Barnes, 1959  
*Biscutum coronum* Wind and Wise in Wise and Wind, 1977  
*Biscutum dissimilis* Wind and Wise in Wise and Wind, 1977  
*Biscutum ellipticum* (Górka, 1957) Grün in Grün and Allemann, 1975  
*Biscutum melaniae* (Górka, 1957) Burnett, 1997a  
*Biscutum notaculum* Wind and Wise in Wise and Wind, 1977  
*Braarudosphaera africana* Stradner, 1961  
*Braarudosphaera bigelowii* (Gran and Braarud, 1935) Deflandre, 1947  
*Braarudosphaera turbinea* Stradner, 1963  
*Broinsonia enormis* (Shumenko, 1968) Manivit, 1971  
*Broinsonia furtiva* Bukry, 1969  
*Broinsonia matalosa* (Stover, 1966) Burnett in Gale et al., 1996  
*Broinsonia parca* (Stradner, 1963) Bukry, 1969, ssp. *constricta* Hattner et al., 1980  
*Broinsonia parca* (Stradner, 1963) Bukry, 1969, ssp. *parca*  
*Broinsonia signata* (Noël, 1969) Noël, 1970  
*Broinsonia verecundia* Wind and Wise in Wise and Wind, 1977  
*Bukrylithus ambiguus* Black, 1971  
*Calciosolenia fossilis* (Deflandre in Deflandre and Fert, 1954) Bown in Kennedy et al., 2000  
*Calculites percenis* Jeremiah, 1996  
*Ceratolithoides* Bramlette and Martini, 1964  
*Ceratolithoides aculeus* (Stradner, 1961) Prins and Sissingh in Sissingh, 1977  
*Ceratolithoides amplexor* Burnett, 1997b  
*Ceratolithoides arcuatus* Prins and Sissingh in Sissingh, 1977  
*Ceratolithoides brevicorniculans* Burnett, 1997b  
*Ceratolithoides indiensis* Burnett, 1997b  
*Ceratolithoides kamptneri* Bramlette and Martini, 1964  
*Ceratolithoides longissimus* Burnett, 1997b  
*Ceratolithoides perangustus* sp. nov.  
*Ceratolithoides pricei* Burnett, 1997b  
*Ceratolithoides prominens* Burnett, 1997b  
*Ceratolithoides quasiarcuatus* Burnett, 1997b  
*Ceratolithoides sagittatus* sp. nov.  
*Ceratolithoides self-trailiae* Burnett, 1997b  
*Ceratolithoides sesquipedalis* Burnett, 1997b  
*Ceratolithoides ultimus* Burnett, 1997b  
*Ceratolithoides verbeekii* Perch-Nielsen, 1979  
*Chiastozygus* Gartner, 1968

*Chiastozygus litterarius* (Górka, 1957) Manivit, 1971  
*Chiastozygus platyrhethus* Hill, 1976  
*Chiastozygus trabalis* (Górka, 1957) Burnett, 1997a  
*Corollithion completum* Perch-Nielsen, 1973  
*Corollithion exiguum* Stradner, 1961  
*Corollithion? madagaskarensis* Perch-Nielsen, 1973  
*Corollithion signum* Stradner, 1963  
*Crepidolithus* Noël, 1965  
*Cretarhabdus conicus* Bramlette and Martini, 1964  
*Cretarhabdus striatus* (Stradner, 1963) Black, 1973  
*Cribracorona echinus* (Bukry, 1975) comb. nov.  
*Cribracorona gallica* (Stradner, 1963) Perch-Nielsen, 1973  
*Cribrospharella ehrenbergii* (Arkhangelsky, 1912) Deflandre in Piveteau, 1952  
*Cyclagelosphaera argoensis* Bown, 1992  
*Cyclagelosphaera deflandrei* (Manivit, 1966) Roth, 1973  
*Cyclagelosphaera margerelii* Noël, 1965  
*Cyclagelosphaera reinhardtii* (Perch-Nielsen, 1968) Romein, 1977  
*Cyclagelosphaera rotaclypeata* Bukry, 1969  
*Cylindralithus* Bramlette and Martini, 1964  
*Cylindralithus nudus* Bukry, 1969  
*Cylindralithus sculptus* Bukry, 1969  
*Cylindralithus serratus* Bramlette and Martini, 1964  
*Cylindralithus? nieliae* Burnett, 1997a  
*Diazomatolithus lehmanii* Noël, 1965  
*Discorhabdus ignotus* (Górka, 1957) Perch-Nielsen, 1968  
*Eiffellithus* Reinhardt, 1965  
*Eiffellithus eximius* (Stover, 1966) Perch-Nielsen, 1968  
*Eiffellithus gorkae* Reinhardt, 1965  
*Eiffellithus monechiae* Crux, 1991  
*Eiffellithus parallelus* Perch-Nielsen, 1973  
*Eiffellithus turriseiffelii* (Deflandre in Deflandre and Fert, 1954) Reinhardt, 1965  
*Eiffellithus windii* Applegate and Bergen, 1988  
*Eiffellithus? hancockii* Burnett, 1997a  
*Eprolithus apertior* Black, 1973  
*Eprolithus floralis* (Stradner, 1962) Stover, 1966  
*Eprolithus moratus* (Stover, 1966) Burnett, 1998  
*Eprolithus octopetalus* Varol, 1992  
*Flabellites oblongus* (Bukry, 1969) Crux in Crux et al., 1982  
*Gartnerago nanum* Thierstein, 1974  
*Gartnerago obliquum* (Stradner, 1963) Noël, 1970  
*Gartnerago ponticulus* **Bown**, this volume  
*Gartnerago segmentatum* (Stover, 1966) Thierstein, 1974  
*Gartnerago stenostaurion* (Hill, 1976) **Bown**, this volume  
*Gartnerago theta* (Black in Black and Barnes, 1959) Jakubowski, 1986  
*Gorkaea operio* Varol and Girgis, 1994  
*Grantarhabdus coronadventis* (Reinhardt, 1966) Grün in Grün and Allemann, 1975  
*Haqius circumradiatus* (Stover, 1966) Roth, 1978  
*Hayesites irregularis* (Thierstein in Roth and Thierstein, 1972) Applegate et al. in Covington and Wise, 1987  
*Helenea chiesta* Worsley, 1971  
*Helicolithus anceps* (Górka, 1957) Noël, 1970  
*Helicolithus compactus* (Bukry, 1969) Varol and Girgis, 1994  
*Helicolithus trabeculatus* (Górka, 1957) Verbeek, 1977  
*Hexalithus gardetiae* Bukry, 1969  
*Kamptnerius magnificus* Deflandre, 1959  
*Lapideacassis* Black, 1971  
*Lapideacassis asymmetrica* (Perch-Nielsen in Perch-Nielsen and Franz, 1977) Burnett, 1997a  
*Lapideacassis cornuta* (Forchheimer and Stradner, 1973) Wind and Wise in Wise and Wind, 1977

*Lapideacassis mariae* Black, 1971  
*Lapideacassis tricornus* Wind and Wise in Wise and Wind, 1977  
*Lithastrinus grillii* Stradner, 1962  
*Lithastrinus quadricuspis* Farhan, 1987  
*Lithastrinus septenarius* Forchheimer, 1972  
*Lithraphidites acutus* Verbeek and Manivit in Manivit et al., 1977  
*Lithraphidites alatus* Thierstein in Roth and Thierstein, 1972  
*Lithraphidites carniolensis* Deflandre, 1963  
*Lithraphidites praequadratus* Roth, 1978  
*Lithraphidites pseudoquadratus* Crux, 1981  
*Lithraphidites quadratus* Bramlette and Martini, 1964  
*Loxolithus* Noël, 1965  
*Loxolithus armilla* (Black in Black and Barnes, 1959) Noël, 1965  
*Loxolithus thiersteinii* (Roth, 1973) comb. nov.  
*Manivitella pemmatoidea* (Deflandre in Manivit, 1965) Thierstein, 1971  
*Markalius inversus* (Deflandre in Deflandre and Fert, 1954) Bramlette and Martini, 1964  
*Microrhabdulus belgicus* Haye and Towe, 1963  
*Microrhabdulus decoratus* Deflandre, 1959  
*Microrhabdulus helicoideus* Deflandre, 1959  
*Microrhabdulus undosus* Perch-Nielsen, 1973  
*Micula* Vekshina, 1959  
*Micula adumbrata* Burnett, 1997a  
*Micula clypeata* sp. nov.  
*Micula cubiformis* Forchheimer, 1972  
*Micula murus* (Martini, 1961) Bukry, 1973  
*Micula praemurus* (Bukry, 1973) Stradner and Steinmetz, 1984  
*Micula premolisilvae* sp. nov.  
*Micula prinsii* Perch-Nielsen, 1979  
*Micula staurophora* (Gardet, 1955) Stradner, 1963  
*Micula swastica* Stradner and Steinmetz, 1984  
*Misceomarginatus pleniporus* Wind and Wise in Wise and Wind, 1977  
*Nannoconus* Kamptner, 1931  
*Neocrepidolithus cohenii* (Perch-Nielsen, 1968) Perch-Nielsen, 1984  
*Nephrolithus* Górka, 1957  
*Nephrolithus frequens* Górka, 1957  
*Octolithus multiplus* (Perch-Nielsen, 1973) Romein, 1979  
*Owenia dispar* (Varol in Al-Rifaiy et al., 1990) Bown in Kennedy et al., 2000  
*Perchnielsenella stradneri* (Perch-Nielsen, 1973) Watkins in Watkins and Bowdler, 1984  
*Petrobrasiella? bownii* Burnett, 1997a  
*Placozygus fibuliformis* (Reinhardt, 1964) Hoffmann, 1970  
*Prediscosphaera arkhangel'skyi* (Reinhardt, 1965) Perch-Nielsen, 1984  
*Prediscosphaera columnata* (Stover, 1966) Perch-Nielsen, 1984  
*Prediscosphaera cretacea* (Arkhangelsky, 1912) Gartner, 1968  
*Prediscosphaera grandis* Perch-Nielsen, 1979  
*Prediscosphaera incohatus* (Stover, 1966) Burnett, 1998  
*Prediscosphaera majungae* Perch-Nielsen, 1973  
*Prediscosphaera microrhabdulina* Perch-Nielsen, 1973  
*Prediscosphaera ponticula* (Bukry, 1969) Perch-Nielsen, 1984  
*Prediscosphaera spinosa* (Bramlette and Martini, 1964) Gartner, 1968  
*Prediscosphaera stoveri* (Perch-Nielsen, 1968) Shafik and Stradner, 1971  
*Prolatipatella multicarinata* Gartner, 1968  
*Pseudomicula quadrata* Perch-Nielsen in Perch-Nielsen et al., 1978  
*Quadrum* Prins and Perch-Nielsen in Manivit et al., 1977  
*Quadrum bengalensis* Burnett, 1998a  
*Quadrum eneabrachium* Varol, 1992  
*Quadrum eptabrachium* Varol, 1992  
*Quadrum gartneri* Prins and Perch-Nielsen in Manivit et al., 1977  
*Quadrum giganteum* Varol, 1992  
*Quadrum intermedium* Varol, 1992

*Quadrum octobrachium* Varol, 1992  
*Quadrum svabenickae* Burnett, 1997a  
*Radiolithus hollandicus* Varol, 1992  
*Radiolithus planus* Stover, 1966  
*Reinhardtites anthophorus* (Deflandre, 1959) Perch-Nielsen, 1968  
*Reinhardtites levis* Prins and Sissingh in Sissingh, 1977  
*Repagulum parvidentatum* (Deflandre and Fert, 1954) Forchheimer, 1972  
*Retecapsa angustiforata* Black, 1971  
*Retecapsa crenulata* (Bramlette and Martini, 1964) Grün in Grün and Allemann, 1975  
*Retecapsa ficula* (Stover, 1966) Burnett, 1997a  
*Retecapsa schizobrachiata* (Gartner, 1968) Grün in Grün and Allemann, 1975  
*Retecapsa surirella* (Deflandre and Fert, 1954) Grün in Grün and Allemann, 1975  
*Rhagodiscus achlyostaurion* (Hill, 1976) Doeven, 1983  
*Rhagodiscus angustus* (Stradner, 1963) Reinhardt, 1971  
*Rhagodiscus asper* (Stradner, 1963) Reinhardt, 1967  
*Rhagodiscus gallagheri* Rutledge and Bown, 1996  
*Rhagodiscus indistinctus* Burnett, 1997a  
*Rhagodiscus plebeius* Perch-Nielsen, 1968  
*Rhagodiscus reniformis* Perch-Nielsen, 1973  
*Rhagodiscus splendens* (Deflandre, 1953) Verbeek, 1977  
*Rotelapillus* Noël, 1973  
*Rotelapillus biarcus* (Bukry, 1969) comb. nov.  
*Rotelapillus crenulatus* (Stover, 1966) Perch-Nielsen, 1984  
*Rucinolithus* Stover, 1966  
*Rucinolithus hayi* Stover, 1966  
*Rucinolithus? magnus* Bukry, 1975  
*Semihololithus dens* Burnett, 1997a  
*Seribiscutum gaultensis* Mutterlose, 1992  
*Seribiscutum primitivum* (Thierstein, 1974) Filewicz et al. in Wise and Wind, 1977  
*Sollasites horticus* (Stradner et al. in Stradner and Adamiker, 1966) Cepek and Hay, 1969  
*Staurolithites* Caratini, 1963  
*Staurolithites? aenigma* Burnett, 1997a  
*Staurolithites* cf. *S. angustus* (Stover, 1966) Crux, 1991  
*Staurolithites crux* (Deflandre and Fert, 1954) Caratini, 1963  
*Staurolithites flavus* Burnett, 1997a  
*Staurolithites gausorhethium* (Hill, 1976) Varol and Girgis, 1994  
*Staurolithites glaber* (Jeremiah, 1996) Burnett, 1997a  
*Staurolithites imbricatus* (Gartner, 1968) Burnett, 1997a  
*Staurolithites laffittei* Caratini, 1963  
*Staurolithites minutus* Burnett, 1997a  
*Staurolithites mutterlosei* Crux, 1989  
*Stoverius achylosus* (Stover, 1966) Perch-Nielsen, 1986  
*Tegumentum* Thierstein in Roth and Thierstein, 1972  
*Tegumentum lucidum* sp. nov.  
*Tegumentum stradneri* Thierstein in Roth and Thierstein, 1972  
*Tetrapodorhabdus decorus* (Deflandre in Deflandre and Fert, 1954) Wind and Wise in Wise and Wind, 1977  
*Thoracosphaera operculata* Bramlette and Martini, 1964  
*Thoracosphaera saxea* Stradner, 1961  
*Tortolithus pagei* (Bukry, 1969) Crux in Crux et al., 1982  
*Tranolithus gabalus* Stover, 1966  
*Tranolithus minimus* (Bukry, 1969) Perch-Nielsen, 1984  
*Tranolithus orionatus* (Reinhardt, 1966a) Reinhardt, 1966b  
*Tubodiscus burnettiae* Bown in Kennedy et al., 2000  
*Uniplanarius* Hattner and Wise, 1980  
*Uniplanarius clarkei* sp. nov.  
*Uniplanarius gothicus* (Deflandre, 1959) Hattner and Wise, 1980  
*Uniplanarius sissinghii* Perch-Nielsen, 1986

- Uniplanarius trifidus* (Stradner in Stradner and Papp, 1961) Hattner and Wise, 1980  
*Watznaueria barnesiae* (Black, 1959) Perch-Nielsen, 1968  
*Watznaueria bayackii* Worsley, 1971  
*Watznaueria biporta* Bukry, 1969  
*Watznaueria britannica* (Stradner, 1963) Reinhardt, 1964  
*Watznaueria fossacincta* (Black, 1971) Bown in Bown and Cooper, 1989  
*Watznaueria manivittiae* Bukry, 1973  
*Watznaueria ovata* Bukry, 1969  
*Watznaueria quadriradiata* Bukry, 1969  
*Zeugrhabdotus bicrescenticus* (Stover, 1966) Burnett in Gale et al., 1996  
*Zeugrhabdotus biperforatus* (Gartner, 1968) Burnett, 1997a  
*Zeugrhabdotus clarus* **Bown**, this volume  
*Zeugrhabdotus diplogrammus* (Deflandre in Deflandre and Fert, 1954) Burnett in Gale et al., 1996  
*Zeugrhabdotus embergeri* (Noël, 1958) Perch-Nielsen, 1984  
*Zeugrhabdotus erectus* (Deflandre in Deflandre and Fert, 1954) Reinhardt, 1965  
*Zeugrhabdotus howei* Bown in Kennedy et al., 2000 (? = *Zeugrhabdotus noeliae* Rood et al., 1971)  
*Zeugrhabdotus praesigmoides* Burnett, 1997a  
*Zeugrhabdotus pseudanthophorus* (Bramlette and Martini, 1964) Perch-Nielsen, 1984  
*Zeugrhabdotus scutula* (Bergen, 1994) Rutledge and Bown, 1996  
*Zeugrhabdotus sigmoides* (Bramlette and Sullivan, 1961) Bown and Young, 1997  
*Zeugrhabdotus spiralis* (Bramlette and Martini, 1964) Burnett, 1997a  
*Zeugrhabdotus trivectis* Bergen, 1994  
*Zeugrhabdotus xenotus* (Stover, 1966) Burnett in Gale et al., 1996

Figure F1. Bathymetric map of Shatsky Rise and location of Shatsky Rise in the Pacific Ocean (insert), relative to other Cretaceous volcanic features. Location of ODP and DSDP sites on Shatsky Rise indicated by filled circles. Modified from Bralower, Premoli Silva, Malone, et al. (2002), Klaus and Sager (2002), and Robinson et al. (2004).

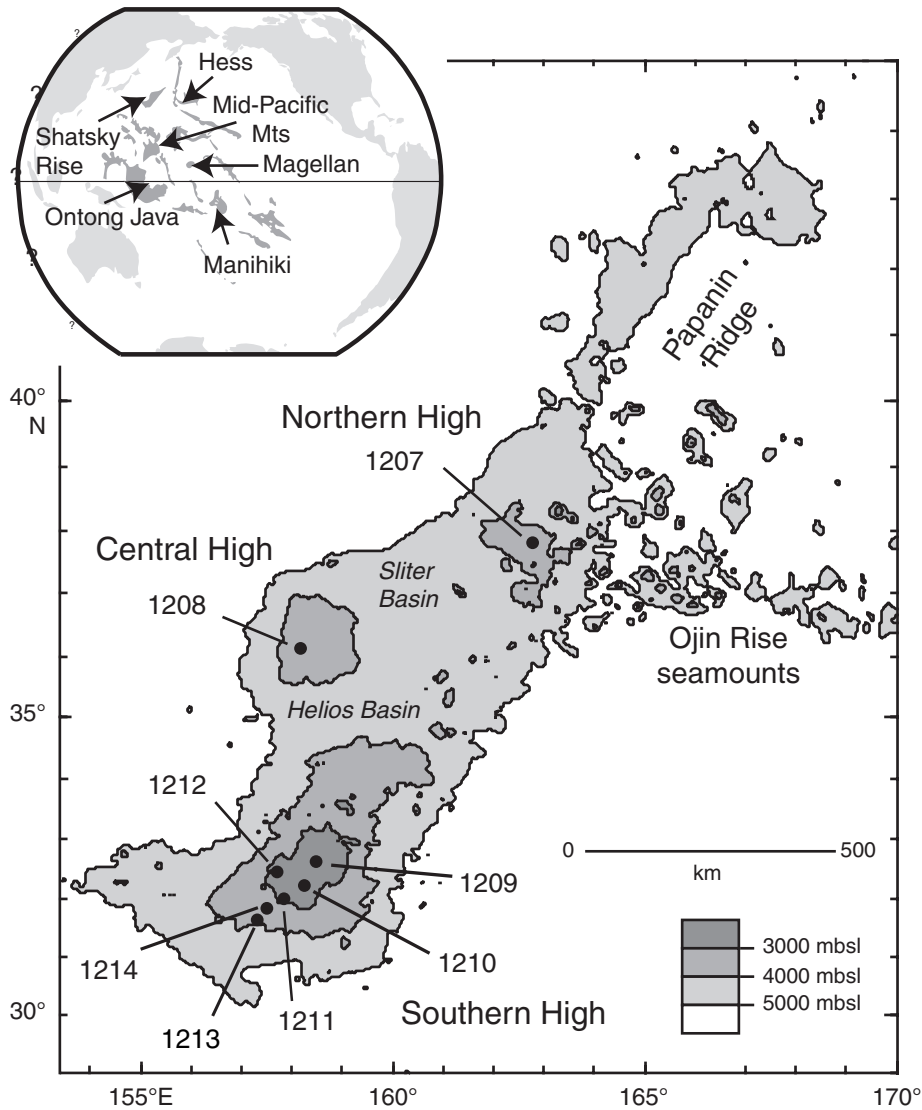


**Figure F2.** Correlation of nannofossil (sub)zones between Shatsky Rise sites. Bold entries = (sub)zonal markers as used in interpreting biostratigraphy.

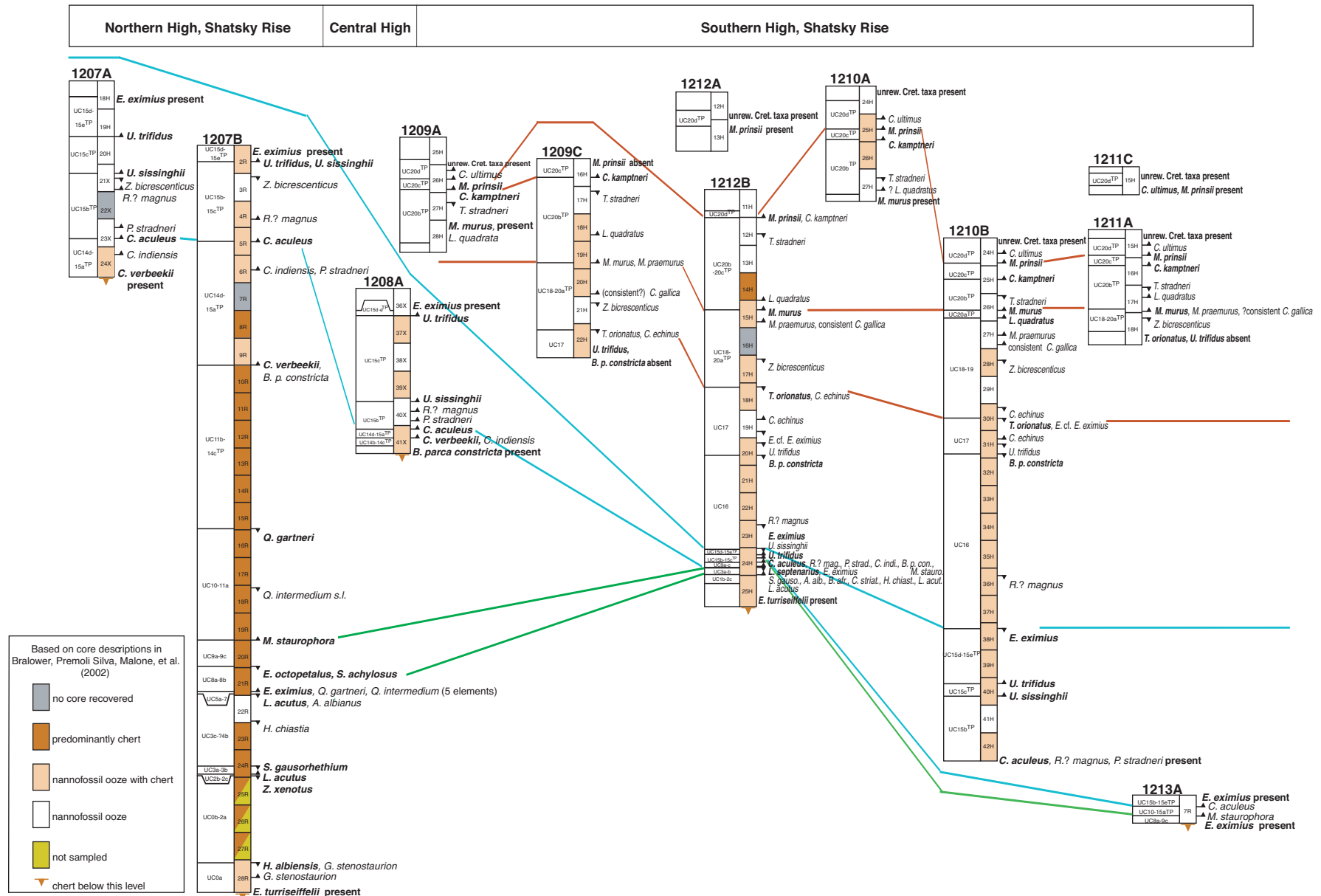


**Table T1.** Calcareous nannofossil stratigraphic range chart, Hole 1207A. (This table is available in an **over-sized format**.)

**Table T2.** Calcareous nannofossil stratigraphic range chart, Hole 1207B. (This table is available in an **over-sized format**.)

**Table T3.** Calcareous nannofossil stratigraphic range chart, Hole 1208A. (This table is available in an [over-sized format](#).)

**Table T4.** Calcareous nannofossil stratigraphic range chart, Hole 1209A. (This table is available in an **over-sized format**.)

**Table T5.** Calcareous nannofossil stratigraphic range chart, Hole 1209C. (This table is available in an **over-sized format**.)

**Table T6.** Calcareous nannofossil stratigraphic range chart, Hole 1210A. (This table is available in an **over-sized format**.)

Table T7. Calcareous nannofossil stratigraphic range chart, Hole 1210B. (This table is available in an [over-sized format](#).)

**Table T8.** Calcareous nannofossil stratigraphic range chart, Hole 1211A. (This table is available in an **over-sized format**.)

**Table T9.** Calcareous nannofossil stratigraphic range chart, Hole 1211C. (This table is available in an **over-sized format**.)

Table T10. Calcareous nannofossil stratigraphic range chart, Hole 1212A. (This table is available in an [over-sized format](#).)

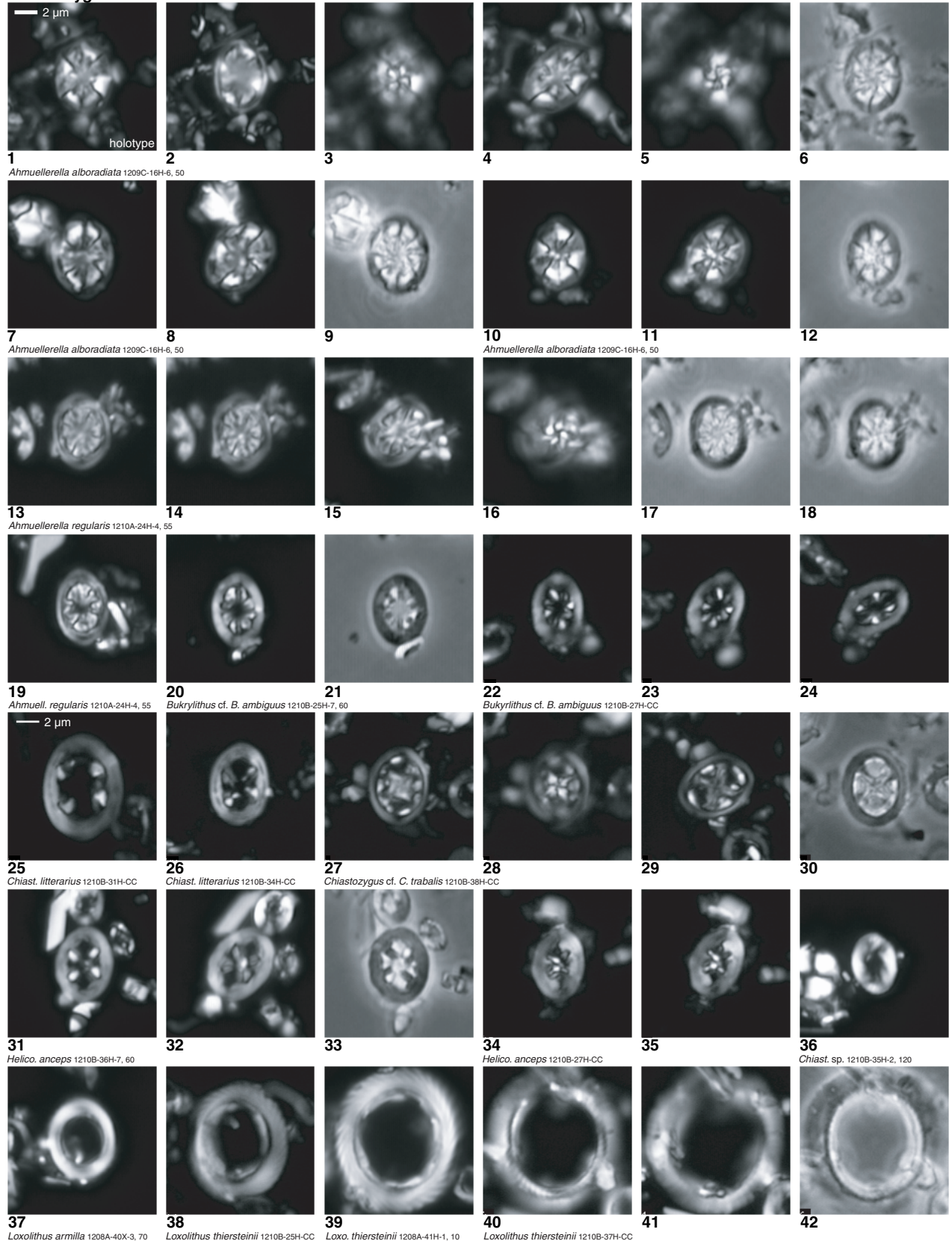
Table T11. Calcareous nannofossil stratigraphic range chart, Hole 1212B. (This table is available in an [over-sized format](#).)

Table T12. Calcareous nannofossil stratigraphic range chart, Hole 1213A. (This table is available in an [over-sized format](#).)

**Plate P1.** Chiasozygaceae. **1–12.** *Ahmuellerella alboradiata*; (1) holotype (Sample 198-1209C-16H-6, 50 cm), (2–12) Sample 198-1209C-16H-6, 50 cm. **13–19.** *Ahmuellerella regularis* (Sample 198-1210A-24H-4, 55 cm). **20–24.** *Bukryolithus* cf. *B. ambiguus*; (20, 21) Sample 198-1210B-25H-7, 60 cm, (22–24) Sample 198-1210B-27H-CC. **25, 26.** *Chiasozygus litterarius*; (25) Sample 198-1210B-31H-CC, (26) Sample 198-1210B-34H-CC. **27–30.** *Chiasozygus* cf. *C. trabalis* (Sample 198-1210B-38H-CC). **31–35.** *Helicolithus anceps*; (31–33) Sample 198-1210B-36H-7, 60 cm, (34, 35) Sample 198-1210B-27H-CC. **36.** *Chiasozygus* sp. (Sample 198-1210B-35H-2, 120 cm). **37.** *Loxolithus amilla* (Sample 198-1208A-40X-3, 70 cm). **38–42.** *Loxolithus thiersteinii*; (38) Sample 198-1210B-25H-CC, (39) Sample 198-1208A-41H-1, 10 cm, (40–42) Sample 198-1210B-37H-CC. (Plate shown on next page.)

Plate P1 (continued). (Caption shown on previous page.)

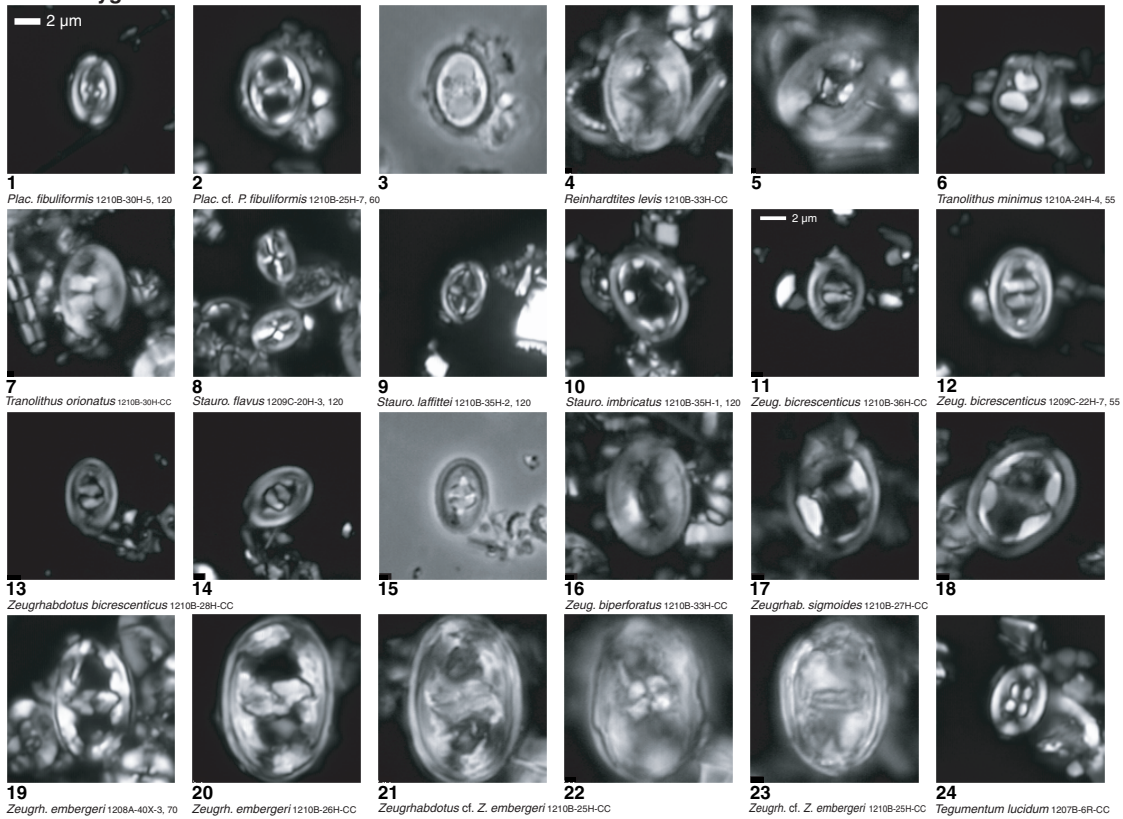
Chiastozygaceae



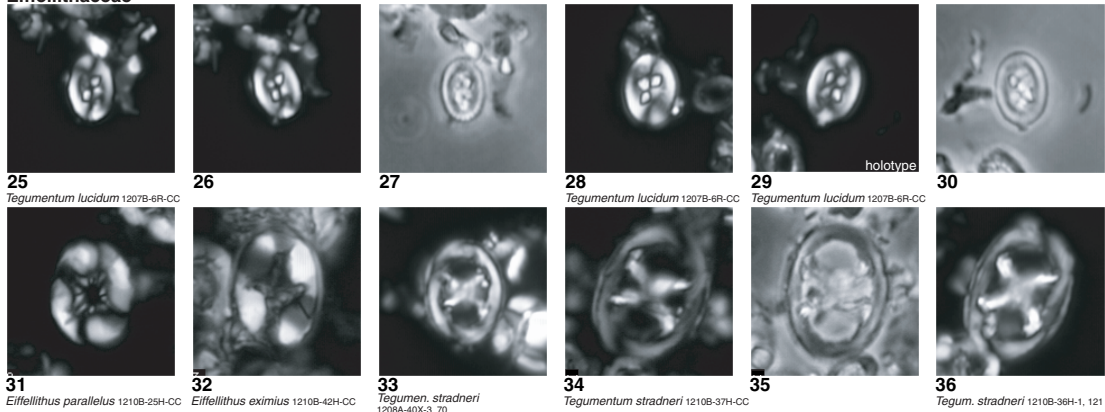
**Plate P2.** Chiastozygaceae, Eiffellithaceae, Rhagodiscaceae. 1. *Placozygus fibuliformis* (Sample 198-1210B-30H-5, 12 cm). 2, 3. *Placozygus* cf. *P. fibuliformis* (Sample 198-1210B-25H-7, 60 cm). 4, 5. *Reinhardtites levis* (Sample 198-1210B-33H-CC). 6. *Tranolithus minimus* (Sample 198-1210A-24H-4, 55 cm). 7. *Tranolithus orionatus* (Sample 198-1210B-30H-CC). 8. *Staurolithites flavus* (Sample 198-1209C-20H-3, 120 cm). 9. *Staurolithites laffittei* (Sample 198-1210B-35H-2, 120 cm). 10. *Staurolithites imbricatus* (Sample 198-1210B-35H-1, 120 cm). 11–15. *Zeugrhabdotus bicrescenticus*; (11) Sample 198-1210B-36H-CC, (12) Sample 198-1209C-22H-7, 55 cm, (13–15) Sample 198-1210B-28H-CC. 16. *Zeugrhabdotus biperforatus* (Sample 198-1210B-33H-CC). 17, 18. *Zeugrhabdotus sigmoides* (Sample 198-1210B-27H-CC). 19, 20. *Zeugrhabdotus embergeri*; (19) Sample 198-1208A-40X-3, 70 cm, (20) Sample 198-1210B-26H-CC. 21–23. *Zeugrhabdotus* cf. *Z. embergeri* (Sample 198-1210B-25H-CC). 24–30. *Tegumentum lucidum*; (24–30) Sample 198-1207B-6R-CC, (29) holotype. 31. *Eiffellithus parallelus* (Sample 198-1210B-25H-CC). 32. *Eiffellithus eximius* (Sample 198-1210B-42H-CC). 33–36. *Tegumentum stradneri*; (33) Sample 198-1208A-40X-3, 70 cm, (34, 35) Sample 198-1210B-37H-CC, (36) Sample 198-1210B-36H-1, 12 cm. 37. *Rhagodiscus angustus* (Sample 198-1209C-19H-1, 21 cm). 38–45. *Rhagodiscus indistinctus*; (38, 43–45) Sample 198-1210B-27H-CC, (39–42) Sample 198-1210B-30H-5, 120 cm. 46. *Rhagodiscus splendens* (Sample 198-1210B-35H-1, 120 cm). 47, 48. *Rhagodiscus reniformis*; (47) Sample 198-1210B-25H-CC, (48) Sample 198-1209C-19H-1, 21 cm. (Plate shown on next page.)

Plate P2 (continued). (Caption shown on previous page.)

**Chiastozygaceae**



**Eiffellithaceae**



**Rhagodiscaceae**

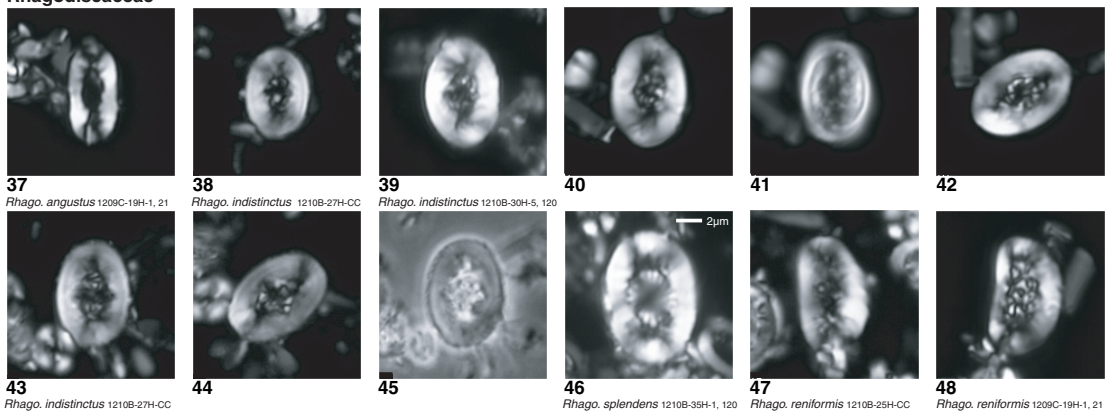
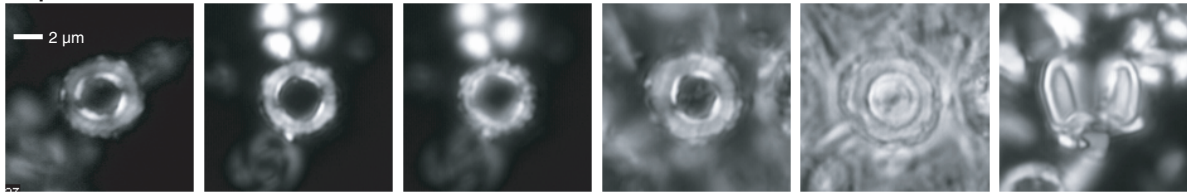


**Plate P3.** Stephanolithiaceae, Axopodorhabdaceae, Biscutaceae, Prediscosphaeraceae. **1–3.** *Rotelapillus biarcus*; (1) Sample 198-1210B-27H-CC, (2, 3) Sample 198-1210B-36H-7, 60 cm. **4–6.** *Rotelapillus* cf. *R. biarcus* (Sample 198-1208A-40X-3, 70 cm). **7.** *Axopodorhabdus dietzmannii* (Sample 198-1210B-25H-CC). **8, 9.** *Tetrapodorhabdus decorus*; (8) Sample 198-1209C-19H-1, 21 cm, (9) Sample 198-1210B-36H-CC. **10, 11.** *Discorhabdus ignotus* (Sample 198-1210B-40H-1, 60 cm). **12–18.** *Discorhabdus* sp. (Sample 198-1209C-18H-5, 50 cm). **19.** *Prediscosphaera spinosa* (Sample 198-1210B-28H-CC). **20.** *Prediscosphaera cretacea* (Sample 198-1210B-42H-CC). **21.** *Prediscosphaera* cf. *P. grandis* (Sample 198-1210B-28H-CC). **22.** *Prediscosphaera grandis* (Sample 198-1210B-24H-4, 50 cm). **23–36.** *Prediscosphaera majungae*; (23, 24) Sample 198-1210B-31H-CC, (25–28) Sample 198-1210B-37H-CC, (29, 30, 36) Sample 198-1210B-30H-CC, (31–34) Sample 198-1210B-42H-CC, (35) Sample 198-1210B-34H-CC. **37, 38.** *Prediscosphaera stoveri* (Sample 198-1210B-40H-1, 60 cm). **39–42.** *Prediscosphaera* spine top; (39, 40) Sample 198-1210B-32H-CC, (41) Sample 198-1210B-42H-CC, (42) Sample 198-1208A-41H-1, 10 cm. (**Plate shown on next page.**)

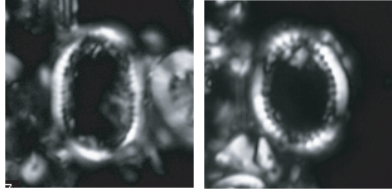
Plate P3 (continued). (Caption shown on previous page.)

**Stephanolithiaceae**



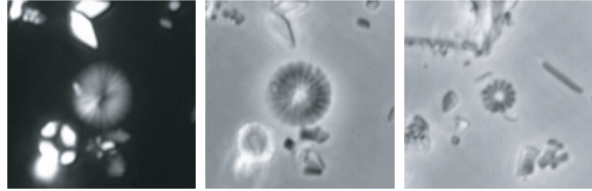
**1** *Rotelapillus biarcus* 1210B-27H-CC    **2** *Rotelapillus biarcus* 1210B-36H-7, 60    **3** *Rotelapillus biarcus* 1210B-36H-7, 60  
**4** *Rotelapillus* cf. *R. biarcus* 1208A-40X-3, 70    **5** *Rotelapillus* cf. *R. biarcus* 1208A-40X-3, 70    **6** *Rotel.* cf. *R. biarcus* 1208A-40X-3, 70

**Axopodorhabdaceae**

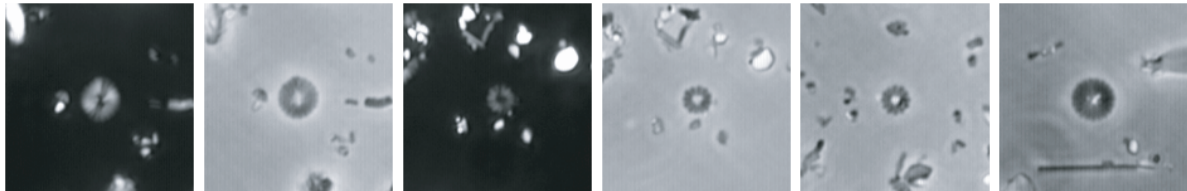


**7** *Axopod. dietzmannii* 1210B-25H-CC    **8** *Tetrapod. decorus* 1209C-19H-1, 21    **9** *Tetrapod. decorus* 1210B-36H-CC

**Biscutaceae**

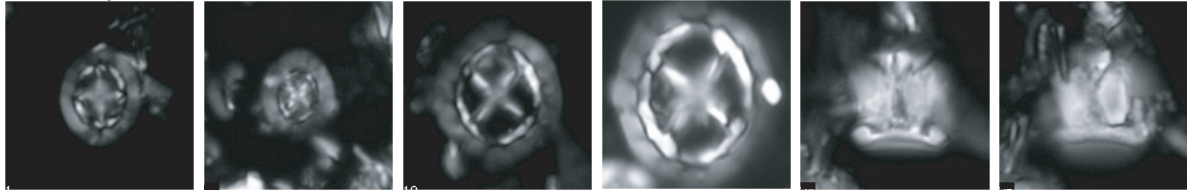


**10** *Discorhabdus ignotus* 1210B-40H-1, 60    **11** *Discorhabdus* sp. 1209C-18H-5, 50    **12** *Discorhabdus* sp. 1209C-18H-5, 50

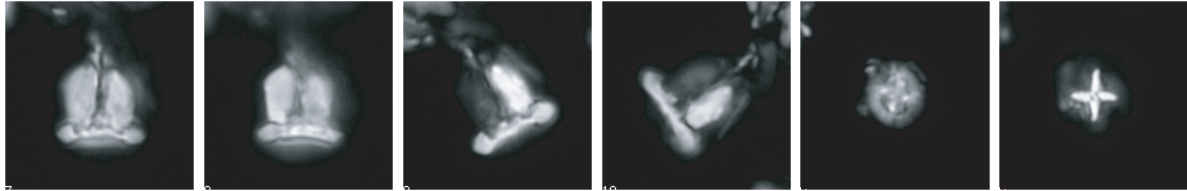


**13** *Discorhabdus* sp. 1209C-18H-5, 50    **14** *Discorhabdus* sp. 1209C-18H-5, 50    **15** *Discorhabdus* sp. 1209C-18H-5, 50    **16** *Discorhabdus* sp. 1209C-18H-5, 50    **17** *Discorhabdus* sp. 1209C-18H-5, 50    **18** *Discorhabdus* sp. 1209C-18H-5, 50

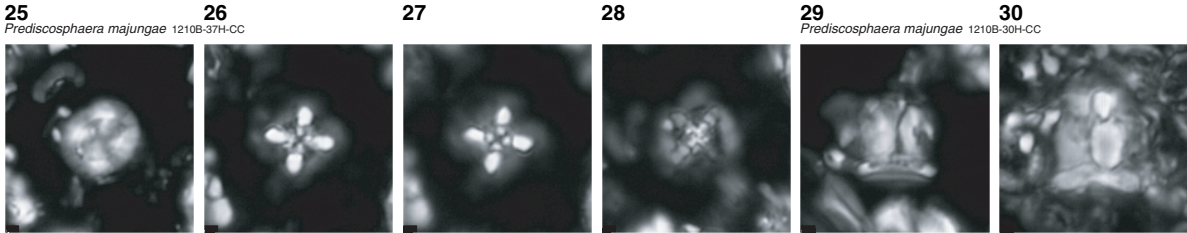
**Prediscosphaeraceae**



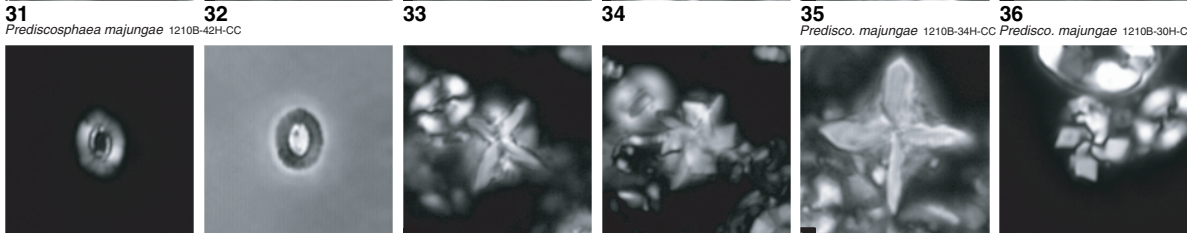
**19** *Predisco. spinosa* 1210B-26H-CC    **20** *Predisco. cretacea* 1210B-42H-CC    **21** *Pred.* cf. *P. grandis* 1210B-28H-CC    **22** *Pred. grandis* 1210B-24H-4, 50    **23** *Prediscosphaera majungae* 1210B-31H-CC    **24** *Prediscosphaera majungae* 1210B-31H-CC



**25** *Prediscosphaera majungae* 1210B-37H-CC    **26** *Prediscosphaera majungae* 1210B-37H-CC    **27** *Prediscosphaera majungae* 1210B-37H-CC    **28** *Prediscosphaera majungae* 1210B-37H-CC    **29** *Prediscosphaera majungae* 1210B-30H-CC    **30** *Prediscosphaera majungae* 1210B-30H-CC



**31** *Prediscosphaera majungae* 1210B-42H-CC    **32** *Prediscosphaera majungae* 1210B-42H-CC    **33** *Prediscosphaera majungae* 1210B-42H-CC    **34** *Prediscosphaera majungae* 1210B-42H-CC    **35** *Predisco. majungae* 1210B-34H-CC    **36** *Predisco. majungae* 1210B-30H-CC

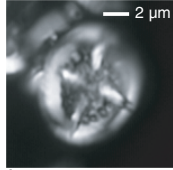


**37** *Prediscosphaera stoveri* 1210B-40H-1, 60    **38** *Prediscosphaera stoveri* 1210B-40H-1, 60    **39** *Prediscosphaera* spine top 1210B-32H-CC    **40** *Prediscosphaera* spine top 1210B-32H-CC    **41** *Predisco.* spine top 1210B-42H-CC    **42** *Predisco.* spine top 1208A-41H-1, 10

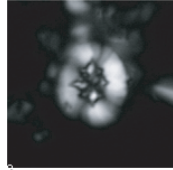
**Plate P4.** Cretarhabdaceae, Watznaueriaceae, *Cribracorona*. **1.** *Cretarhabdus conicus* (Sample 198-1210B-39H-4, 60 cm). **2.** *Retecapsa angustiforata* (Sample 198-1210B-34H-CC). **3.** *Retecapsa ficula* (Sample 198-1209C-19H-1, 21 cm). **4, 5.** *Retecapsa schizobrachiata*; (4) Sample 198-1210B-27H-CC, (5) Sample 198-1210B-34H-5, 45 cm. **6.** *Retecapsa surirella* (Sample 198-1210B-36H-1, 121 cm). **7.** *Cylindralithus nudus* (Sample 198-1210B-26H-CC). **8, 9.** *Cylindralithus serratus* (Sample 198-1210B-25H-CC). **10–18.** *Cylindralithus sculptus*; (10–12, 16, 17) Sample 198-1208A-41H-1, 40 cm, (13–15, 18) Sample 198-1208A-41H-1, 100 cm. **19–21.** *Cylindralithus? nieliae* (Sample 198-1210B-36H-1, 121 cm). **22–30.** *Perchnielsenella stradneri*; (22, 23) Sample 198-1209C-20H-3, 120 cm, (24) Sample 198-1210B-42H-CC, (25–28) Sample 198-1209C-22H-7, 55 cm, (29, 30) Sample 198-1210B-28H-CC. **31–41.** *Cribracorona echinus*; (31, 32, 38, 39, 41) Sample 198-1210B-30H-CC, (33–37, 40) Sample 198-1210B-30H-5, 120 cm. **42–48.** *Cribracorona gallica* (Sample 198-1210B-24H-2, 75 cm). (Plate shown on next page.)

Plate P4 (continued). (Caption shown on previous page.)

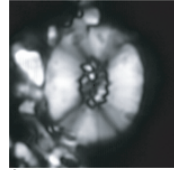
**Cretarhabdaceae**



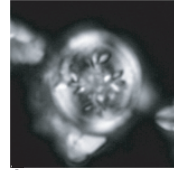
1 *Cretarhab. conicus* 1210B-39H-4, 60



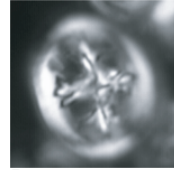
2 *Rete. angustiflora* 1210B-34H-CC



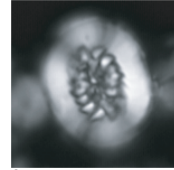
3 *Retecapsa ficula* 1209C-19H-1, 21



4 *Ret. schizobrachiata* 1210B-27H-CC

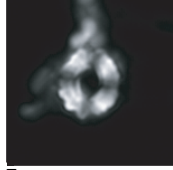


5 *Ret. schizobrachiata* 1210B-34H-5, 45

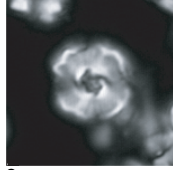


6 *Retecapsa surirella* 1210B-36H-1, 121

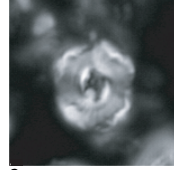
**Watznaueriaceae**



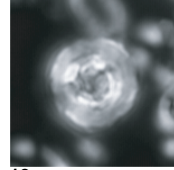
7 *Cylindralithus nudus* 1210B-26H-CC



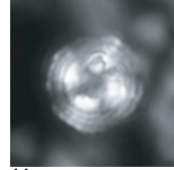
8 *Cylindralithus serratus* 1210B-25H-CC



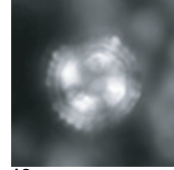
9 *Cylindralithus serratus* 1210B-25H-CC



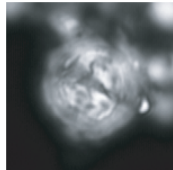
10 *Cylindralithus sculptus* 1208A-41H-1, 40



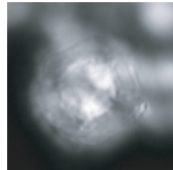
11 *Cylindralithus sculptus* 1208A-41H-1, 40



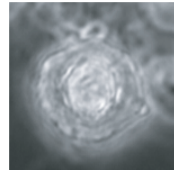
12 *Cylindralithus sculptus* 1208A-41H-1, 40



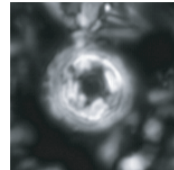
13 *Cylindralithus sculptus* 1208A-41H-1, 100



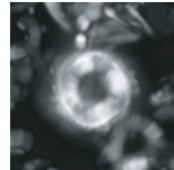
14 *Cylindralithus sculptus* 1208A-41H-1, 100



15 *Cylindralithus sculptus* 1208A-41H-1, 100



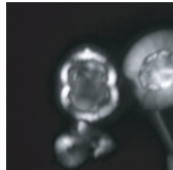
16 *Cylindralithus sculptus* 1208A-41H-1, 40



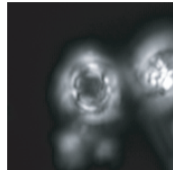
17 *Cylindralithus sculptus* 1208A-41H-1, 40



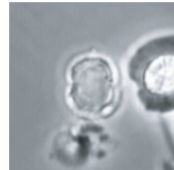
18 *Cylindralithus sculptus* 1208A-41H-1, 100



19 *Cylindralithus? nielae* 1210B-36H-1, 121



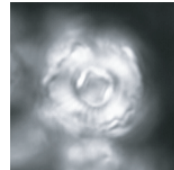
20 *Cylindralithus? nielae* 1210B-36H-1, 121



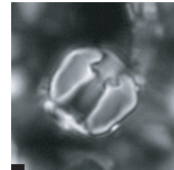
21 *Perchnielsenella stradneri* 1209C-20H-3, 120



22 *Perchnielsenella stradneri* 1209C-20H-3, 120



23 *Perchnielsenella stradneri* 1209C-22H-7, 55



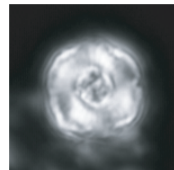
24 *Perchnielsenella stradneri* 1210B-42H-CC



25 *Perchnielsenella stradneri* 1209C-22H-7, 55



26 *Perchnielsenella stradneri* 1209C-22H-7, 55



27 *Perchnielsenella stradneri* 1209C-22H-7, 55



28 *Perchnielsenella stradneri* 1209C-22H-7, 55

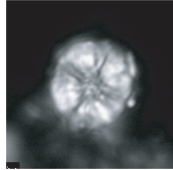


29 *Perchnielsenella stradneri* 1210B-28H-CC

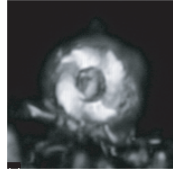


30 *Perchnielsenella stradneri* 1210B-28H-CC

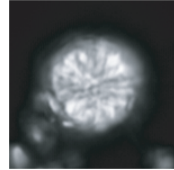
**Cribracorona**



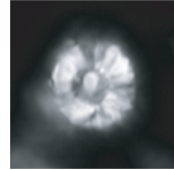
31 *Cribracorona echinus* 1210B-30H-CC



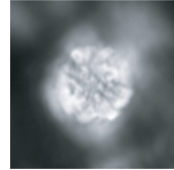
32 *Cribracorona echinus* 1210B-30H-5, 120



33 *Cribracorona echinus* 1210B-30H-5, 120



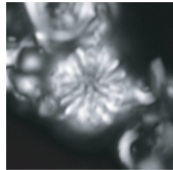
34 *Cribracorona echinus* 1210B-30H-5, 120



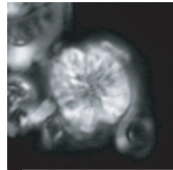
35 *Cribracorona echinus* 1210B-30H-5, 120



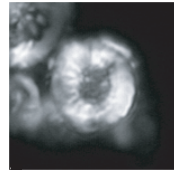
36 *Cribracorona echinus* 1210B-30H-5, 120



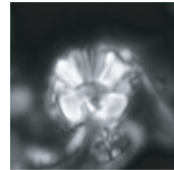
37 *Cribracorona echinus* 1210B-30H-5, 120



38 *Cribracorona echinus* 1210B-30H-CC



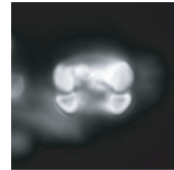
39 *Cribracorona echinus* 1210B-30H-5, 120



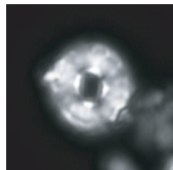
40 *Cribracorona echinus* 1210B-30H-5, 120



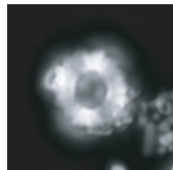
41 *Cribracorona echinus* 1210B-30H-CC



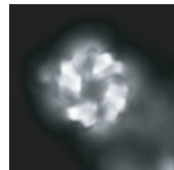
42 *Cribracorona gallica* 1210B-24H-2, 75



43 *Cribracorona gallica* 1210B-24H-2, 75



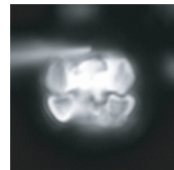
44 *Cribracorona gallica* 1210B-24H-2, 75



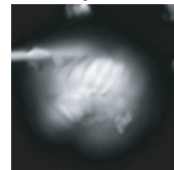
45 *Cribracorona gallica* 1210B-24H-2, 75



46 *Cribracorona gallica* 1210B-24H-2, 75



47 *Cribracorona gallica* 1210B-24H-2, 75

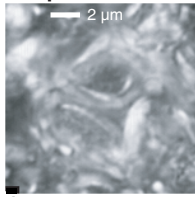


48 *Cribracorona gallica* 1210B-24H-2, 75

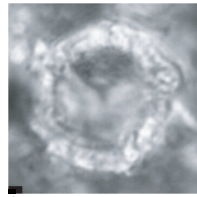
**Plate P5.** Axopodorhabdaceae, Tubodiscaceae, Arkhangelskiellaceae, Kampteriaceae, Nannoliths. **1–4.** *Cribrosphaerella ehrenbergii*; (1, 2) Sample 198-1210B-35H-CC, (3, 4) Sample 198-1212B-21H-1, 120 cm. **5, 6.** *Manivitella pemmatoidea*; (5) Sample 198-1210B-28H-CC, (6) Sample 198-1210B-37H-CC. **7.** *Broinsonia* cf. *B. furtiva* (Sample 198-1210B-30H-CC). **8–12.** *Broinsonia parca constricta*; (8–10) Sample 198-1210B-37H-CC, (11) Sample 198-1210B-36H-1, 121 cm, (12) Sample 198-1210B-35H-CC. **13, 14.** *Arkhangelskiella confusa*; (13) Sample 198-1210B-31H-CC, (14) Sample 198-1210B-29H-CC. **15–17.** *Arkhangelskiella cymbiformis*; (15, 16) Sample 198-1210B-27H-CC, (17) Sample 198-1210B-26H-CC. **18.** *Gartnerago segmentatum* (Sample 198-1209C-20H-3, 120 cm). **19–21.** *Assipetra terebrodentarius*; (19) Sample 198-1208A-41H-1, 10 cm, (20, 21) Sample 198-1208A-41H-1, 100 cm. **22–24.** *Braarudosphaera turbinea*; (22, 23) Sample 198-1208A-41H-1, 40 cm, (24) Sample 198-1208A-41H-1, 10 cm. **25.** *Lapideacassis mariae* (Sample 198-1210B-27H-CC). **26.** *Lapideacassis asymmetrica* (Sample 198-1210B-29H-CC). **27.** *Lapideacassis* sp. (Sample 198-1210B-30H-5, 120 cm). **28–31.** *Lithraphidites quadratus*; (28, 29) Sample 198-1210B-25H-7, 60 cm, (30) Sample 198-1210B-24H-CC, (31) Sample 198-1210B-24H-4, 45 cm. **32, 33.** *Microrhabdulus decoratus* (Sample 198-1210B-31H-CC). **34–36.** *Pseudomicula quadrata*; (34) Sample 198-1210B-24H-4, 65 cm, (35, 36) Sample 198-1210B-24H-2, 75 cm. **37.** UFO1 (Sample 198-1208A-41H-1, 100 cm). **38–40.** UFO2; (38, 40) Sample 198-1210B-24H-CC, (39) Sample 198-1210B-38H-CC. **41, 42.** Blades; (41) Sample 198-1210B-24H-4, 45 cm, (42) Sample 198-1210B-24H-5, 5 cm. (Plate shown on next page.)

Plate P5 (continued). (Caption shown on previous page.)

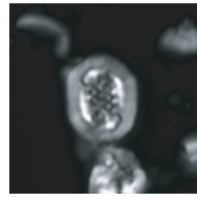
**Axopodorhabdaceae**



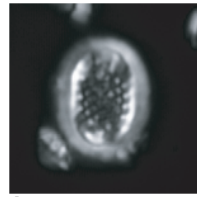
1 *Cribro. ehrenbergii* 1210B-35H-CC



2



3 *Cribro. ehrenbergii* 1212B-21H-1, 120

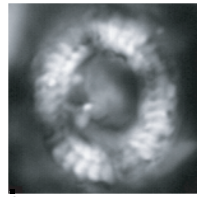


4 *Cribro. ehrenbergii* 1212B-21H-1, 120

**Tubodiscaceae**

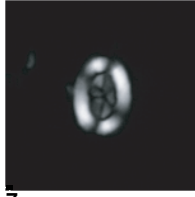


5 *Manivit. pemmatoidea* 1210B-28H-CC

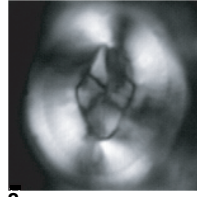


6 *Manivit. pemmatoidea* 1210B-37H-CC

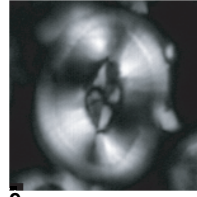
**Arkhangelskiellaceae**



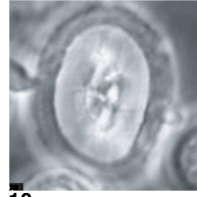
7 *Broin. cf. B. furtiva* 1210B-30H-CC



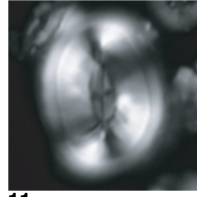
8 *Broin. p. constricta* 1210B-37H-CC



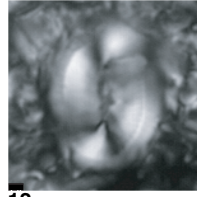
9 *Broin. p. constricta* 1210B-37H-CC



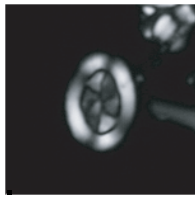
10



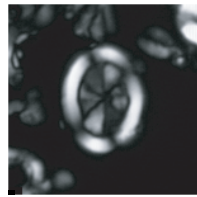
11 *Broin. p. constricta* 1210B-36H-1, 121



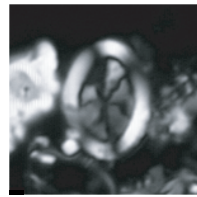
12 *Broin. p. constricta* 1210B-35H-CC



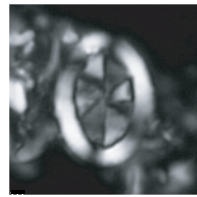
13 *Arkhang. confusa* 1210B-31H-CC



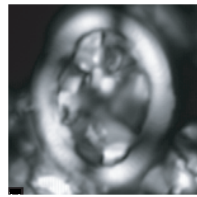
14 *Arkhang. confusa* 1210B-29H-CC



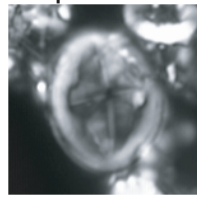
15 *Arkhang. cymbiformis* 1210B-27H-CC



16 *Arkhang. cymbiformis* 1210B-27H-CC

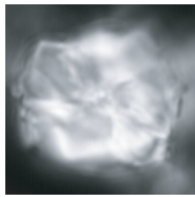


17 *Arkhang. cymbiformis* 1210B-26H-CC

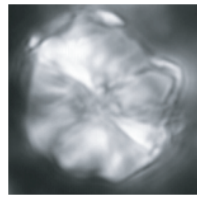


18 *Gart. segmentatum* 1209C-20H-3, 120

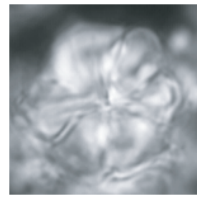
**Kamptneriaceae**



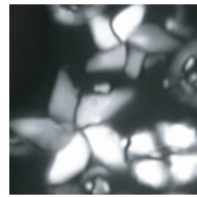
19 *A. terebrodentarius* 1208A-41H-1, 10



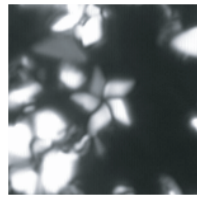
20 *A. terebrodentarius* 1208A-41H-1, 100



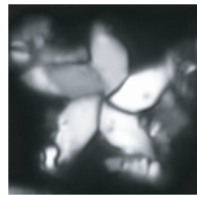
21 *A. terebrodentarius* 1208A-41H-1, 100



22 *Braarudo. turbinea* 1208A-41H-1, 40



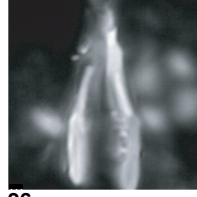
23 *Braarudo. turbinea* 1208A-41H-1, 40



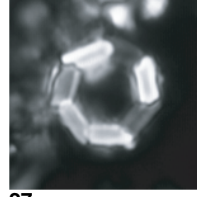
24 *Braarudo. turbinea* 1208A-41H-1, 10



25 *Lapideacassis mariae* 1210B-27H-CC



26 *Lapid. asymmetrica* 1210B-29H-CC



27 *Lapideacassis* sp. 1210B-30H-5, 120



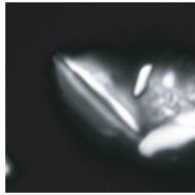
28 *Lithraphidites quadratus* 1210B-25H-7, 60



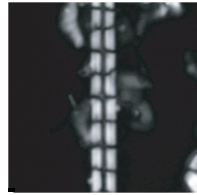
29



30 *Lithraphidites quadratus* 1210B-24H-CC



31 *Lithraph. quadratus* 1210B-24H-4, 45



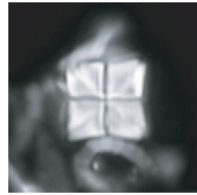
32 *Microrhabdulus decoratus* 1210B-31H-CC



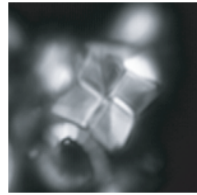
33



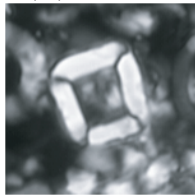
34 *Pseudom. quadrata* 1210B-24H-4, 65



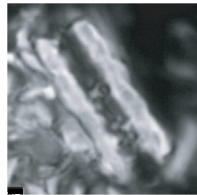
35 *Pseudomicula quadrata* 1210B-24H-2, 75



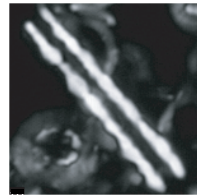
36



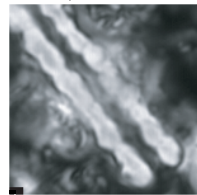
37 UFO1 1208A-41H-1, 100



38 UFO2 1210B-24H-CC



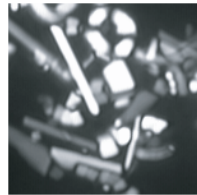
39 UFO2 1210B-38H-CC



40 UFO2 1210B-24H-CC



41 blades 1210B-24H-4, 45



42 blades 1210B-24H-5, 5

**Plate P6.** *Ceratolithoides*. 1. *Ceratolithoides aculeus* (Sample 198-1210B-37H-CC). 2, 3. *Ceratolithoides amplector*; (2) Sample 198-1210B-24H-CC, (3) Sample 198-1210B-25H-CC. 4–6. *Ceratolithoides* cf. *C. amplector*; (4) Sample 198-1210B-38H-CC, (5) Sample 198-1210B-25H-7, 60 cm, (6) Sample 198-1210B-26H-CC. 7–11. *Ceratolithoides indiensis*; (7, 9) Sample 198-1210B-25H-CC, (8, 11) Sample 198-1210B-35H-1, 120 cm, (10) Sample 198-1210B-30H-5, 120 cm. 12–18. *Ceratolithoides longissimus*; (12–14) Sample 198-1210B-32H-7, 72 cm, (15) Sample 198-1210B-32H-CC, (16–18) Sample 198-1210B-31H-CC. 19, 20. *Ceratolithoides* cf. *C. longissimus*; (19) Sample 198-1210B-31H-CC, (20) Sample 198-1210B-36H-7, 60 cm. 21–23. *Ceratolithoides perangustus*; (21) Sample 198-1210B-36H-CC, (22) holotype (Sample 198-1210B-36H-7, 60 cm), (23) Sample 198-1210B-36H-7, 60 cm. 24. *Ceratolithoides pricei* (Sample 198-1210B-25H-7, 60 cm). 25–30. *Ceratolithoides sagittatus*; (25) Sample 198-1210B-36H-CC, (26) holotype (Sample 198-1210B-38H-CC), (27, 29) Sample 198-1210B-38H-CC, (28) Sample 198-1210B-40H-1, 60 cm, (30) Sample 198-1210B-42H-CC. 31–33. *Ceratolithoides self-trailiae*; (31) Sample 198-1210B-26H-CC, (32) Sample 198-1210B-27H-CC, (33) Sample 198-1210B-25H-7, 60 cm. 34–36. *Ceratolithoides ultimus*; (34) Sample 198-1210A-24H-4, 55 cm, (35, 36) Sample 198-1210A-24H-4, 65 cm. 37–42. *Ceratolithoides verbeekii* (Sample 198-1207B-6R-CC). (Plate shown on next page.)

Plate P6 (continued). (Caption shown on previous page.)

*Ceratolithoides*



**Plate P7.** Polycyclolithaceae–*Micula*. 1–3. *Micula adumbrata* (Sample 198-1209C-16H-6, 50 cm). 4–6. *Micula cubiformis* (Sample 198-1210B-25H-CC). 7–12. *Micula murus*; (7, 8) Sample 198-1210B-24H-2, 75 cm, (9, 10) Sample 198-1210B-24H-4, 45 cm, (11, 12) Sample 198-1210A-24H-4, 55 cm. 13–22. *Micula* cf. *M. murus*; (13–15, 19, 20) Sample 198-1210B-24H-CC, (16–18) Sample 198-1209C-22H-7, 55 cm, (21) side view (Sample 198-1210B-28H-CC), (22) side view (Sample 198-1210B-27H-CC). 23, 24. *Micula staurophora*; (23) Sample 198-1209C-18H-7, 50 cm, (24) Sample 198-1210B-30H-5, 120 cm. 25–33. *Micula swastica*; (25–27, 31–33) Sample 198-1210B-37H-CC, (28–30) Sample 198-1210B-25H-CC. 34–39. *Micula* cf. *M. swastica* (Sample 198-1210B-25H-CC). 40–42. *Micula swastica?* side view; (40) Sample 198-1210B-25H-CC, (41) Sample 198-1210B-27H-CC, (42) Sample 198-1210B-37H-CC. (Plate shown on next page.)

Plate P7 (continued). (Caption shown on previous page.)

Polycyclolithaceae - *Micula*



**Plate P8.** Polycyclolithaceae–*Micula*. 1–12. *Micula prinsii*; (1–6, 8, 10–12) Sample 198-1210A-24H-4, 55 cm, (7) Sample 198-1210B-24H-4, 45 cm, (9) Sample 198-1210B-24H-4, 1 cm. 13–21. *Micula praemurus* (Sample 198-1210B-26H-CC). 22–30. *Micula premolisilvae*; (22–24, 29) Sample 198-1210B-32H-CC, (25) holotype (Sample 198-1210B-34H-CC), (26) Sample 198-1210B-34H-CC, (27, 28) Sample 198-1210B-36H-CC, (30) Sample 198-1210B-27H-CC. 31–48. *Micula clypeata* (Sample 198-1209C-18H-7, 50 cm); (31) holotype. **(Plate shown on next page.)**

Plate P8 (continued). (Caption shown on previous page.)

Polycyclolithaceae - *Micula*

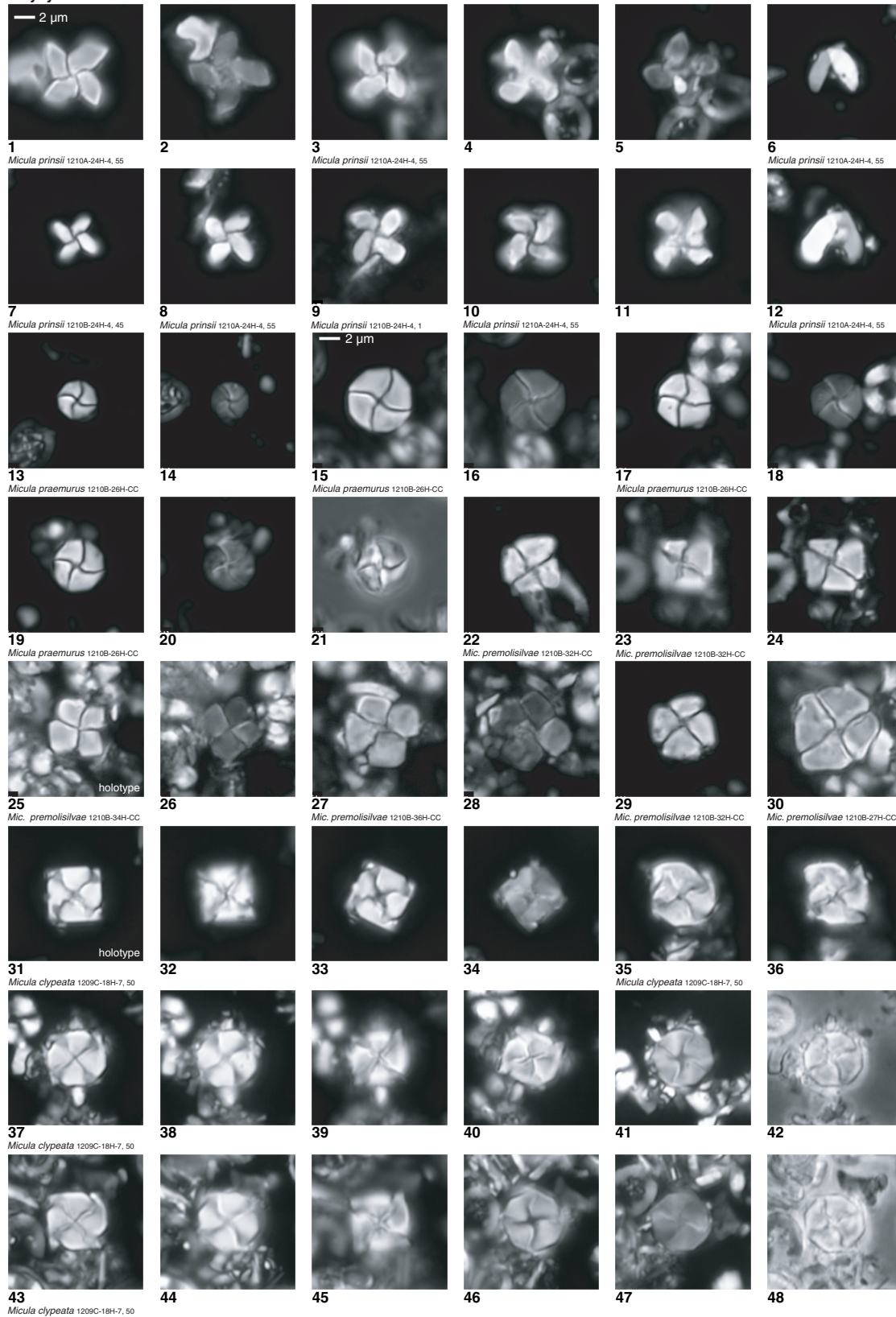


**Plate P9.** Polycyclolithaceae–*Uniplanarius*. 1–12. *Uniplanarius clarkei* (Sample 198-1210B-34H-5, 45 cm); (1) holotype. 13–26. *Uniplanarius gothicus*; (13–18) Sample 198-1210B-40H-1, 60 cm, (19–21) Sample 198-1210B-31H-CC, (22, 23, 25, 26) Sample 198-1210B-37H-CC, (24) Sample 198-1210B-36H-7, 60 cm. 27–30. *Uniplanarius* cf. *U. gothicus* (small); (27) Sample 198-1210B-37H-CC, (28) Sample 198-1210B-42H-CC, (29, 30) Sample 198-1210B-34H-5, 45 cm. 31–36. *Uniplanarius trifidus*; (31–33) Sample 198-1210B-31H-CC, (34) Sample 198-1210B-32H-CC, (35) Sample 198-1210B-33H-CC, (36) Sample 198-1210B-35H-1, 120 cm. 37, 38. *Uniplanarius* cf. *U. sissinghii* (Sample 198-1210B-41H-CC). 39–41. *Uniplanarius sissinghii*; (39, 40) Sample 198-1210B-33H-CC, (41) Sample 198-1210B-32H-CC. 42. *Uniplanarius gothicus?* (Sample 198-1210B-35H-CC). (Plate shown on next page.)

Plate P9 (continued). (Caption shown on previous page.)

Polycyclolithaceae - *Uniplanarius*

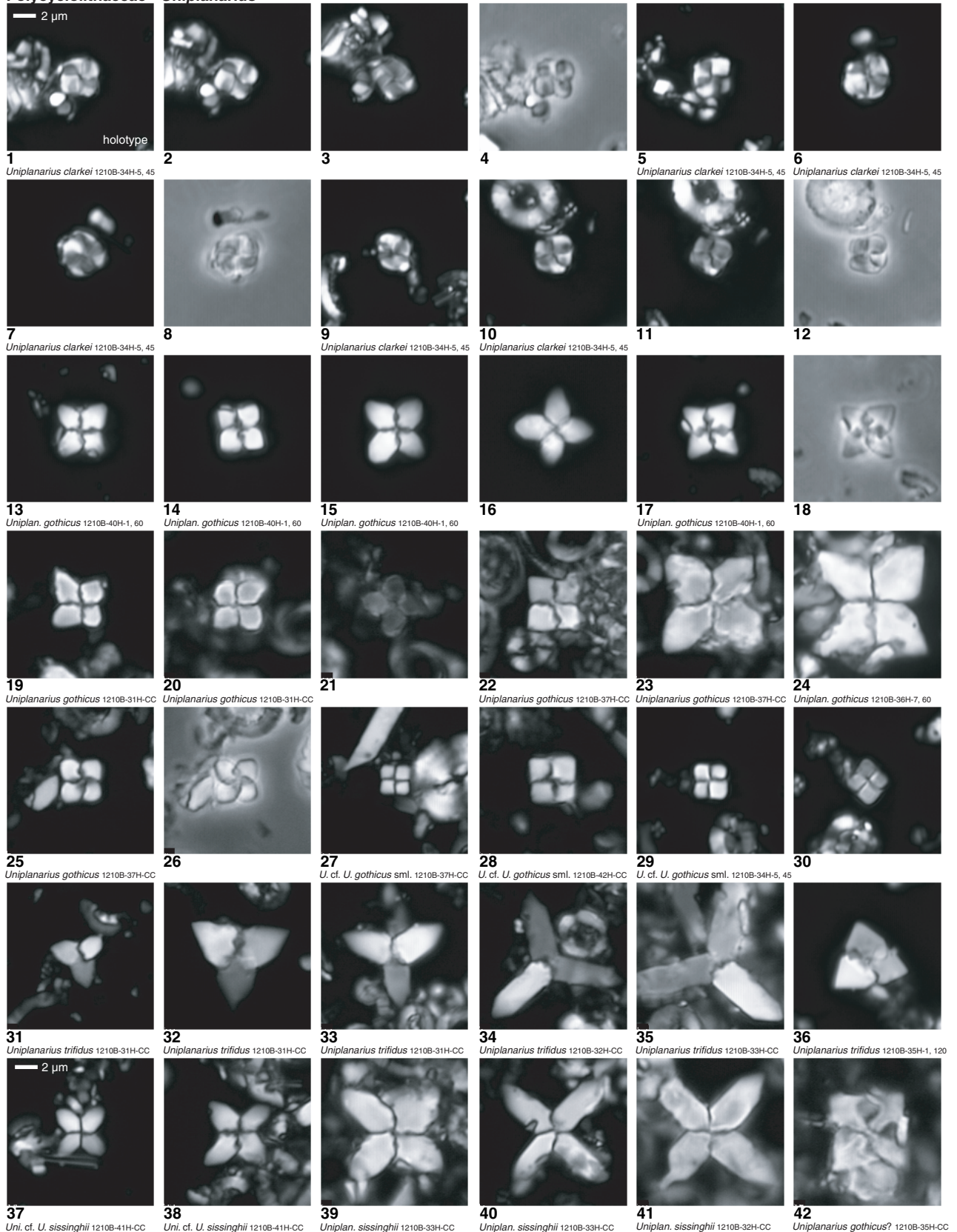


**Plate P10.** Other polycycloliths. **1–4.** *Quadrum svabenickae*; (1, 2) Sample 198-1210B-40H-1, 60 cm, (3, 4) Sample 198-1210B-41H-CC. **5–10.** *Lithastrinus quadricuspis?*; (5, 6) Sample 198-1210B-36H-CC, (7–10) Sample 198-1210B-32H-CC. **11, 12.** *Uniplanarius* cf. *U. sissinghii*; (11) Sample 198-1210B-35H-1, 120 cm, (12) Sample 198-1210B-32H-7, 72 cm. **13–15.** *Lithastrinus grillii* (Sample 198-1208A-41H-1, 100 cm). **16.** *Hexalithus gardetiae* (Sample 198-1210B-36H-7, 60 cm). **17–24.** *Rucinolithus hayi*; (17, 18, 22) Sample 198-1210B-36H-7, 60 cm, (19, 24) Sample 198-1210B-36H-CC, (20, 21) Sample 198-1210B-39H-4, 60 cm. **25–33.** *Rucinolithus? magnus*; (25–28) Sample 198-1208A-40X-3, 70 cm, (29–32) Sample 198-1210B-42H-CC, (33) Sample 198-1208A-40X-3, 70 cm. **34–36.** *Rucinolithus?* sp. (spine top); (34) Sample 198-1210B-27H-CC, (35) Sample 198-1210B-28H-CC, (36) Sample 198-1209C-18H-7, 50 cm. **37.** *Uniplanarius sissinghii* (Sample 198-1210B-32H-CC). **38, 39.** *Uniplanarius trifidus*; (38) Sample 198-1210B-33H-CC, (39) Sample 198-1210B-32H-CC. **40.** UFO2 (Sample 198-1210B-36H-CC). (**Plate shown on next page.**)

Plate P10 (continued). (Caption shown on previous page.)

Other Polycycloliths

